universität wien

MASTERARBEIT / MASTER'S THESIS

Titel der Masterarbeit / Title of the Master's Thesis

„ Evaluation and optimization of the radiotracers [^{18}F]FTHA and [^{68}Ga]Ga-DATA^{5m}.SA.FAPi for positron emission tomography (PET) "

verfasst von / submitted by

Hannah Kanatschnig BSc

angestrebter akademischer Grad / in partial fulfilment of the requirements for the degree of

Master of Science (MSc)

Wien, 2021

Studienkennzahl lt. Studienblatt / degree programme code as it appears on the student record sheet:	A 066 862
Studienrichtung lt. Studienblatt / degree programme as it appears on the student record sheet:	Chemie
Betreut von / Supervisor:	Assoz. Prof. Mag. Dr. Wolfgang Wadsak, Privatdoz.
Mitbetreut von / Co-Supervisor:	Mag. Dr. Cécile Philippe

ACKNOWLEDGEMENTS

Throughout the practical and writing portion of this thesis I have received support and assistance from many people.

I would first like to thank Assoz. Prof. Mag. Dr. Wolfgang Wadsak, Privatdoz. for the opportunity to research in his group.

Special thanks to my supervisor Mag. Dr. Cécile Philippe for the valuable support and always helpful advice.

I would also like to say thank you to the whole research group and all employees of the radiology and nuclear medicine department of the AKH Vienna especially Stefan, Eva and Fritz. The positive and friendly environment was a big help.

In addition, I would like to thank my temporary work partner Sev for the constructive discussions and fun during my practical portion of this work.

My biggest thanks belong to my family Gabriele, Manfred, Hugo, Mira, Felix, Erna, Alex, Gerlinde and Gabi for financial and emotional support throughout my study. It would not have been possible without you.

Another special thanks to my friends, especially Anna, Alex, Sophie, Bella and Angi for the indescribable help you give me. With your kind hearts, you make me a better person every day. Thank you!

I would also like to thank everyone who made my time as a student as unique as it was, whether it was happy free time adventures or studying. I would never want to miss it.

ABSTRACT

Radiolabeled compounds are already used routinely in therapy and diagnostics as well as together in another interesting approach, the theranostic one. Various diseases can be located and treated with compounds that are radiolabeled with different radionuclides. Gallium-68 and fluorine-18 are both positron-emitting radionuclides used for PET imaging and the interest in novel radiopharmaceuticals labeled with those nuclides steadily increases.

The ^{18}F-labeled fatty acid tracer 14-*(R,S)*-[^{18}F]fluoro-6-thia-heptadecanoic acid ([^{18}F]FTHA) is used to investigate β-oxidation and fatty acid metabolism in heart and skeletal muscle. Previous studies showed the successful radiolabeling with an automated synthesis module for fluorine-18. In this work, the radiolabeling was performed manually and then transferred to an automated synthesis module (originally designed for carbon-11 syntheses). The radiolabeling to [^{18}F]FTHA resulted in high radiochemical purities over 99% and decay-corrected (to the end of bombardment) radiochemical yields of 10 ± 3%. To obtain optimized parameters, the focus was set on the subsequent application in animal studies with the necessity to have sufficient radioactivity in 100 µL volumes at the end of the synthesis. The whole process of radiolabeling plus formulation took around 88 minutes. The stability of the radiotracer was determined in a period of 4 hours after synthesis. At room temperature, the tracer showed high stability above 97%. To estimate the behavior *in vivo*, incubation in mouse plasma and human serum, respectively, was performed. After 3 hours, the stability was still above 97% in human serum, but lower in mouse plasma.

A wide range of macrocyclic and acyclic chelators radiolabeled with gallium-68 were studied in previous papers. The radiotracer [^{68}Ga]Ga-DATA^{5m}.SA.FAPi was synthesized in this work. It is a fibroblast activation protein (FAP) inhibitor that binds to the active site of FAP which is overexpressed in tissue remodeling sites like tumors, inflammations, or arthritis. The radiolabeling resulted in radiochemical purities of 97% and above but stability tests showed fast decomposition. Already after 1 h after synthesis the stability was mostly under 95% which is not suitable for long lasting animal studies.

Further *in vivo* and *in vitro* studies are needed to allow the clinical use of the two synthesized radiotracers. However, the clinical potential of both compounds is undisputed.

ZUSAMMENFASSUNG

Heutzutage werden radioaktive Moleküle bereits routiniert verwendet, sei es in der Therapie oder Diagnose. Außerdem sind sie zukunftsorientierte und interessante Herangehensweise in der Sparte Theranostik. Viele unterschiedliche Krankheiten und biologische Vorgänge können durch Verbindungen, die radioaktiv markiert sind, lokalisiert, behandelt oder verfolgt werden. Gallium-68 und Fluor-18 sind Positronen strahlende Isotope, welche für die Bildgebung mittels PET genutzt werden. Das Interesse an neuen Radiopharmaka steigt stetig.

Der mit Fluor-18 markierte Fettsäurestoffwechseltracer 14-*(R,S)*-[^{18}F]Fluor-6-thia-heptadecansäure ([^{18}F]FTHA) wird verwendet, um die β-Oxidation und Fettsäurestoffwechsel im Herzen und Skelettmuskel zu untersuchen. Studien haben bereits die erfolgreiche Radiomarkierung mit automatischen Synthesemodulen, welche spezifisch für Fluor-18 sind, gezeigt. In dieser Arbeit wurde zuerst die Radiomarkierung manuell durchgeführt und zu späterem Zeitpunkt auf ein automatisches Synthesemodul transferiert, welches jedoch für ^{11}C-Radiomarkieungen bestimmt ist. [^{18}F]FTHA wurde erfolgreich synthetisiert mit Zerfall-korrigierten radiochemischen Ausbeuten von 10 ± 3%. Dabei wurde anfangs der Fokus auf die Tierversuche und die Radioaktivität in 100 µL Produkt am Ende der Synthese gelegt. Der gesamte Prozess der Radiomarkierung plus Formulierung dauerte etwa 88 Minuten. Die Stabilität des Radiotracers wurde in einem Zeitraum von 4 Stunden nach der Synthese bestimmt. Bei Raumtemperatur zeigte der Tracer eine hohe Stabilität von über 97%. Um das Verhalten *in vivo* abzuschätzen zu können, wurde er in Mausplasma und Humanserum inkubiert. Nach 3 Stunden lag die Stabilität des Tracers im Humanserum immer noch bei über 97%, im Mausplasma jedoch darunter.

Eine breite Palette makrozyklischer und azyklischer Chelatoren wurde bereits in vielen Studien mit Gallium-68 radioaktiv markiert. In dieser Arbeit wurde der Radiotracer [^{68}Ga]Ga-DATA^{5m}.SA.FAPi synthetisiert. Es handelt sich dabei um einen Fibroblasten-Aktivierungsprotein-Inhibitor, der an die aktive Stelle von FAP bindet, die bei Gewebeumbau wie Tumoren, Entzündungen oder Arthritis übermäßig stark ausgeprägt ist. Die Radiomarkierung führte zu radiochemischen Reinheiten von über 97%, aber Stabilitätstests zeigten eine schnelle Zersetzung. Selbst 1 Stunde nach Synthese lag die Stabilität meist unter 95%, was für länger andauernde Tierversuche nicht geeignet ist.

Weitere *in vivo* und *in vitro* Studien sind nötig, um die beiden hergestellten Radiotracer in den Routinebetrieb der Bildgebung aufzunehmen. Das Potential dieser ist jedoch unumstritten.

TABLE OF CONTENT

ABBREVIATION

[^{18}F]FTHA	*14-(R,S)-[^{18}F]Fluoro-6-thia-heptadecanoic acid*
µg	*Microgram*
µL	*Microliter*
µm	*Mikrometer*
µmol	*Micromol*
^{18}F	*Fluor-18*
^{68}Ga	*Gallium-68*
^{68}Ge	*Germanium-68*
Å	*Ångström*
ACN	*Acetonitrile*
AcOH	*Acetic acid*
AKH	*General hospital*
Bq	*Becquerel*
CH_3COOH	*Acetic acid*
cm	*Centimeter*
DATA	*6-Amino-1,4-diazapine*
DOTA	*2,2',2'',2'''-(1,4,7,10-Tetraazacyclododecane-1,4,7,10-tetrayl)tetraacetic acid*
EtOAc	*Ethyl acetate*
EtOH	*Ethanol*
eV	*Electron volt*
FAP	*Fibroblast activation protein*
FAPi	*Fibroblast activation protein inhibitor*
GBq	*Gigabecquerel*
GC	*Gas chromatography*
GE	*General Electric*
h	*Hour; hours*
H_2O	*Water*
HPLC	*High performance liquid chromatography*
iTLC	*Instant thin layer chromatography*
$K_{2.2.2}$	*Kryptofix ® 222*
K_2CO_3	*Potassium carbonate*
keV	*Kilo electron volt*
KF	*Potassium fluoride*
kg	*Kilogram*
KOH	*Potassium hydroxide*
m	*Minute; minutes*
M	*Molar [mol/L]*
MBq	*Megabecquerel*
MeOH	*Methanol*
MeV	*Mega electron volt*
mg	*Milligram*
min	*Minutes*
mL	*Milliliter*
mm	*Millimeter*
mosmo	*Milliosmolality per liter*
NaCl	*Sodium chloride*
NH_4OAc	*Ammonium acetate*
nm	*Nanometer*

nmol ..... *Nanomol*
PET ..... *Positron emission tomography*
rpm ..... *Revolutions per minute [1/min]*
s ..... *Second; seconds*
SA ..... *Squaric acid*
SPE ..... *Solid phase extraction*
TFA ..... *Trifluoroacetic acid*
TLC ..... *Thin layer chromatography*
UV ..... *Ultraviolet*
v% ..... *Volume percentage*

1 INTRODUCTION

1.1 NUCLEAR AND RADIOCHEMISTRY

1.1.1 RADIOACTIVITY

Radioactivity is the property of unstable nuclei to transform into different nuclei under emission of rays and particles or the capture of electrons.[1] All nuclides with a higher atomic number than bismuth (83) are radioactive. Lead is the heaviest element with stable isotopes known.[2]

1.1.2 RADIOACTIVE DECAY

The transformation of nuclei is characterized by particle emission like in alpha and beta decay or ray emission like in gamma rays and spontaneous fission (Table 1). These decays can take place at the same time in different combinations of the processes and are naturally occuring.[1]

Table 1: Summary of the decay modes.[3]

Decay mode	Particle/Radiation emitted	General reaction	Example
α decay	${}^{4}_{2}\mathrm{He}^{2+}$	${}^{A}_{Z}X \rightarrow {}^{A-4}_{Z-2}Y + {}^{4}_{2}He^{2+}$	${}^{226}_{88}Ra \rightarrow {}^{222}_{86}Rn^{2-} + {}^{4}_{2}He^{2+} + energy$
β^- decay	Electron	${}^{A}_{Z}X \rightarrow {}^{A}_{Z+1}Y + {}^{0}_{-1}e^{-}$	${}^{227}_{89}Ac \rightarrow {}^{227}_{90}Th^{+} + {}^{0}_{-1}e^{-} + energy$
β^+ decay	Positron	${}^{A}_{Z}X \rightarrow {}^{A}_{Z-1}Y + {}^{0}_{1}e^{+}$	${}^{40}_{19}K \rightarrow {}^{40}_{18}Ar^{-} + {}^{0}_{-1}e^{+} + energy$
γ-ray	Photons		
Electron capture		${}^{A}_{Z}X \rightarrow {}^{A}_{Z-1}Y + v_e$	${}^{0}_{-1}e^{-} + {}^{197}_{80}Hg \rightarrow {}^{197}_{79}Au$
Spontaneous fission	Fission fragments, neutrons		${}^{252}_{98}Cf \rightarrow {}^{142}_{56}Ba + {}^{106}_{42}Mo + 4{}^{1}_{0}n$

1.1.2.1 IMPORTANT PARAMETERS OF RADIOACTIVE DECAY

Radioactive decay is time dependent and can be expressed with the half-life of an atom, which describes the time when the half of the radioactive atoms are decayed. The rate can be described with equation (**1**), where N is the number of atoms of the radionuclide and λ is the decay constant. dN is the number of spontaneous transitions from a specific energy level in the time interval dt. This is a rate law of first-order.[3]

$$-\frac{dN}{dt} = \lambda N \qquad (\mathbf{1})$$

With the general mononuclear reaction $X \rightarrow Y + a + \Delta E$ and the relation found by Einstein $\Delta E = \Delta mc^2$, the energy and the possibility of a decay process can be determined. Radioactive decay can only occur when $\Delta E > 0$. Integration of equation (**1**) gives equation (**2**) with N_0 as the number of radioactive atoms at the time 0.[3]

$$N = N_0 e^{-\lambda t} \qquad (\mathbf{2})$$

Instead of the decay constant λ, the half-life $t_{1/2}$ is more frequently used (equation (**3**)), where the number of radioactive atoms are decayed by half: $N_0 e^{-\lambda t_{1/2}} = \frac{N_0}{2}$.[3]

$$t_{1/2} = \frac{\ln 2}{\lambda} \qquad (\mathbf{3})$$

Equation (**4**) shows the calculation of the radioactive activity A, that is proportional to the number of radioactive nuclei N with s^{-1} as dimension, which is equal to Bq (1 Bq = 1 s^{-1} = 1 decay per second).[3]

$$A = -\frac{dN}{dt} = \lambda N = A_0 e^{-\lambda t} = N_0 e^{-\lambda t} \qquad (\mathbf{4})$$

1.1.2.2 α DECAY

During α decay the emission of a helium nucleus with two neutrons and two protons takes place leading to a nucleus of an element with a mass number reduced by four (see equation (**5**)).[2]

$${}^{A}_{Z}X \rightarrow {}^{A-4}_{Z-2}Y + {}^{4}_{2}He^{2+} \qquad (\mathbf{5})$$

1.1.2.3 β DECAY

There are two types of β decay, the β^- and β^+ decay, which are described in this chapter.

1.1.2.3.1 β^- DECAY

The release of an electron leads to an atom with a by one increased atomic number while the mass number remains the same (see equation (**6**)). During β^- decay a neutron in the nucleus transforms into a proton under the release of energy in form of negatively charged electrons and antineutrinos $\bar{\nu}_e$ (see equation (**7**)).[2]

$${}^{A}_{Z}X \rightarrow {}^{A}_{Z+1}Y + {}^{0}_{-1}e^{-} \qquad (\mathbf{6})$$

$$n \rightarrow p^{+} + e^{-} + \bar{\nu}_e \qquad (\mathbf{7})$$

1.1.2.3.2 β^+ DECAY

During β^+ decay the release of a positron leads to a new atom with a by one decreased atomic number while the mass number remains the same (see equation (**8**)). Thereby a proton transforms into a neutron

in the nucleus under the release of a positively charged electron, which is called a positron and a neutrino ν_e (see equation (**9**)).[2]

$$ {}^{A}_{Z}X \rightarrow {}^{A}_{Z-1}Y + {}^{0}_{1}e^{+} \qquad (\mathbf{8}) $$

$$ p^{+} \rightarrow n + e^{+} + \nu_e \qquad (\mathbf{9}) $$

1.1.2.3.3 Electron Capture

During electron capture the nucleus of an atom captures an electron from the inner electron shell (K or L shell) and a proton in the nucleus transforms into a neutron (see equation (**10**)). The atomic number decreases by 1 and the mass is unaltered (see equation (**11**)).[4]

$$ {}^{A}_{Z}X \rightarrow {}^{A}_{Z-1}Y + \nu_e \qquad (\mathbf{10}) $$

$$ p^{+} + e^{-} \rightarrow n + \nu_e \qquad (\mathbf{11}) $$

Through the excitation energy the emission of electromagnetic radiation in form of X-ray or γ-radiation takes place after the electron capture.[5]

1.1.2.4 γ-rays

γ-Rays are electromagnetic radiation with the shortest electromagnetic waves. There is no change in the atomic and mass number. α and β decay are mostly accompanied by γ-rays. The emission of γ-rays occurs when the atomic nucleus of an excited state transits into a state with lower energy.[1]

1.1.2.5 Spontaneous Fission

Another type of radioactive decay is the spontaneous fission. Radionuclides with atomic numbers higher than 230 can also release other nuclei than helium. Nuclei that undergo spontaneous fission split into two fragment nuclei under the emission of neutrons and energy.[2]

1.1.3 Nuclear radiation and their interaction with matter

All different kinds of nuclear radiation have properties that need to be known to measure and identify them. One of the most important aspects is the interaction of radiation with matter.[3,5] The process of ionization or excitation in matter is caused by high-energy particles or photons like α-particles, protons, electrons, positrons or γ-rays with a minimum energy of several eV. Several secondary reactions can occur like recombination, charge transfer, dissociation, fluorescence and many more.[3] The amount of energy that is transferred per unit distance in matter is called linear energy transfer (LET) and it varies from medium to medium (water, air). Additionally, all types of radiation show a different behavior in a

magnetic field with distinction of deflection (Figure 1). The absorption will be discussed in this chapter, but the ratio of α, β and γ with the same energy is 10^4:10^2:1.[3]

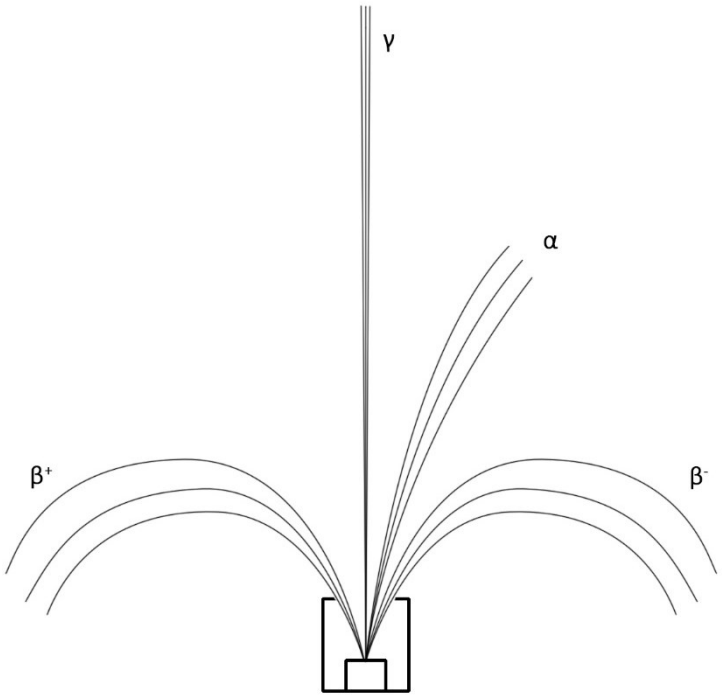

Figure 1: Behavior of different types of radiation.[3]

α-radiation

α-Particles are heavy charged particles with energies ranging from 3 to 10 MeV and the radiation can easily be absorbed by a sheet of paper. In the air thousands of ion pairs per millimeter are produced by an α-particles with the energy of 3 MeV and its range of 1.7 cm.[3,5] They interact with orbital electrons, the nuclear field or rarely with the nucleus. The consequences are ionization, scattering or the initiation of nuclear reactions.[5]

β-radiation

The interaction with matter of β-radiation is much weaker than with α-radiation and the deflection much bigger (Figure 1). Compared to an α-particle, a β-particle with the energy of 3 MeV has a range of 10 meters in the air and produces only around four ion pairs per millimeter. To absorb β-radiation materials with several millimeters or centimeters are necessary.[3] β-radiation interacts with matter causing excitation or ionization, with the nuclear field causing *Bremsstrahlung* or the particles can be scattered and absorbed (Figure 2).[5] When the radiation interacts with orbital electrons of an absorber leading to excitation and ionization, the density of those electrons in the matter is important for the range of these β-particles.[3] The electromagnetic radiation called Cherenkov radiation is also observed during β-radiation when the speed of the β-particles in a dielectric medium is greater than the velocity of light in the matter. This kind of radiation is only possible when the energy of β-particles is a minimum of

0.26 MeV. Another important interaction is the annihilation of positrons during the β^+ decay: If the positron encounters an electron, they transform in 90% of all cases into two γ-photons with energies of 0.51 MeV. Those are emitted in an angle of 180 ° and this property is also used in PET imaging. β-Particles can also be absorbed from the matter and so decrease the intensity of radiation, for example during scattering. When measuring β-radiation, the self-absorption, that is dependent on the thickness of the matter and the energy, is also an influencing factor that can be corrected. Since β-particles are lighter than α-particles, they can scatter on orbital electrons and in the nuclear field. The backscattering can be measured and used to determine some information about the thickness of the matter, the atomic number or the concentration of the solution.[5]

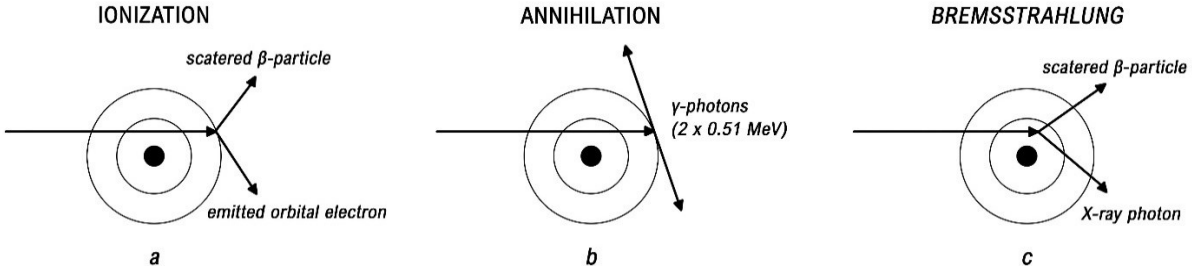

Figure 2: Interaction of β-radiation. a and b: interaction with orbital electrons; c: interaction with nuclear field.[5]

γ-radiation

The energy of γ-rays ranges from 10 keV to 10^4 MeV with wavelengths from 0.1 nm to 10^{-7} nm. For the absorption of γ-radiation, lead or thick concrete is needed.[3] X-rays and γ-rays have similar properties and both are electromagnetic radiation but the produced photons have a different origin. γ-Rays are always emitted from nuclei when changing from excited to lower energy state *versus* x-rays from the inner electron orbitals.[3,5] γ-Photons do not have a mass or charge.[5] There are different effects caused by γ-photons on the matter: the interaction with orbital electrons causing scattering, the photoelectric effect; the Compton effect and the interaction with the nuclear field causing pair formation.[5] During the photoelectric effect a γ-photon transfers its energy to an orbital electron, which is then emitted as photoelectron with the energy $E_k = E_\gamma - E_b$ with E_k as the kinetic energy of the photoelectron, E_γ as the energy of the photon before interaction and E_b as the binding energy of the electron.[3,5] The Compton effect occurs at higher energies, when the photon only transfers part of its energy to an electron *via* inelastic collision. Thereby the γ-photon is deflected and the energy of the scattered γ-photon is $E = \frac{E_0}{1 + q \cdot E_0}$ with E_0 as the initial energy of the photon and q as $\frac{1 - \cos\delta}{m_0 c^2}$ (δ is the scattering angle, m_0 the electron mass and c the velocity of light).[5] The Compton electron has an energy of $E = \frac{q \cdot E_0}{1 + q \cdot E_0}$. There are two other scattering types:[5] the Rayleigh scattering at γ-energies around 100 keV leading to secondary radiation and also the Thomson scattering. In both cases the wavelength of the scattered radiation stays

the same and it is an elastic scattering. The last effect, the pair formation, only occurs at γ-photon energies higher than 1.02 MeV ($2m_0c^2$). Thereby the photon transforms into a positron and an electron. The possibility of pair formation increases with the square of the atomic number of the absorber. All effects summed up give the total absorption of the matter.[3,5]

1.1.4 PRODUCTION OF RADIONUCLIDES

Radionuclides used in nuclear medicine are mostly produced artificially with a cyclotron or radionuclide generator, which are described in this chapter.

1.1.4.1 CYCLOTRON

A cyclotron accelerates charged particles in a spiral-like path shown in Figure 3. It consists of two hollow electrodes, the dees, that are placed in an evacuated chamber between the poles of a magnet. A high frequency alternating voltage *V* connects the dees. The particles, that are produced in the gap by the ion source *A*, are captured by the induced electric field and soaked into the hollow space of the dees. Under the influence of the homogeneous magnetic field the particles move in a semicycle. Everytime they pass the gap, the electric field accelerates them until they reach the desired speed. The radius of the path and the energy of the particles increases with the speed. The deflector *B* deflects the particles so they can reach the target.[2,6]

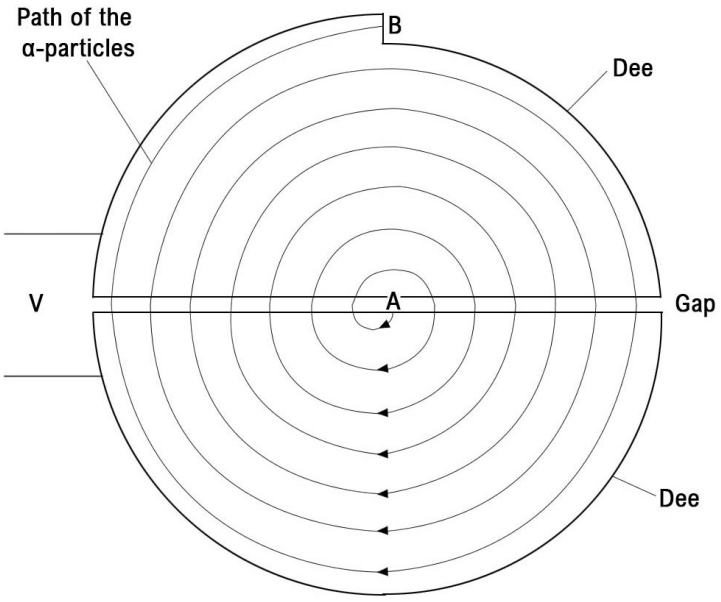

Figure 3: Schematics of a cyclotron. A ion source, B deflector, V alternating voltage.

1.1.4.1.1 FLUORINE-18 PRODUCTION

Fluorine-18 is produced with a cyclotron by the bombardment of a target with protons (^1H). The nuclear reaction is $^{18}O(p,n)^{18}F$. To obtain an aqueous solution of [^{18}F]fluoride ions, the target is enriched water [^{18}O]H_2O and to obtain [^{18}F]F_2 the target is [^{18}O]O_2 gas. Dependent on the desired chemical reaction

(nucleophilic or electrophilic), the different production methods are used. Those are described in more detail in chapter 1.1.5.[7]

1.1.4.2 GENERATOR

Radionuclide generators are used to produce short-lived radionuclides with the help of the parent-daughter radionuclide relationship. In principle, the long-lived parent nuclide decays to the short-lived daughter nuclide and afterwards they get separated. A radioactive equilibrium is the requirement for the function of a generator. One out of the following two conditions needs to be fulfilled: transient equilibrium ($t_{1/2,daughter} < t_{1/2,parent} < 100$), or secular equilibrium ($t_{1/2,daughter} <<< t_{1/2,parent}$). A scheme of the setup is shown in Figure 4. Due to the easy handling, they are frequently used directly in nuclear medicine institutions.[6,8]

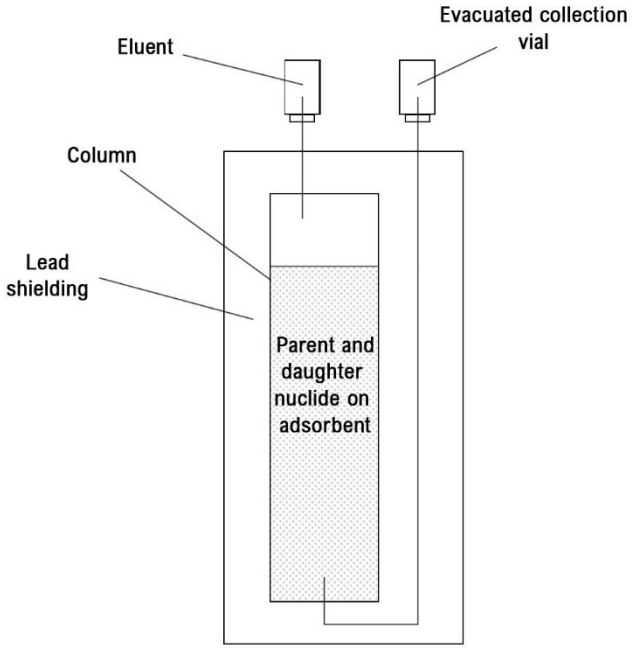

Figure 4: Generator scheme.

1.1.4.2.1 GALLIUM-68 PRODUCTION

Gallium-68 is produced in a $^{68}Ge/^{68}Ga$-generator. The principle of operation is based on the secular equilibrium between the parent radionuclide germanium-68 and its daughter radionuclide gallium-68. The half-life of germanium-68 is 270.95 days and it decays via electron capture to gallium-68, which subsequently decays to zinc-68 with a half-life of 68 minutes. The amount of gallium-68 decaying and producing is equal at equilibrium while the quantity of germanium-68 does not decrease significantly.[8]

The setup of a $^{68}Ge/^{68}Ga$-generator is shown in Figure 4. The parent nuclide is bound to the carrier, mostly titanium(IV)oxide continuously producing the daughter nuclide. Hydrochloric acid is often used

to elute gallium-68 and not germanium-68. The desired gallium-68 elution is transferred to the evacuated collection vial.[6]

1.1.5 RADIOCHEMISTRY OF FLUORINE-18

Fluorine-18 has a half-life of 109.7 min with 97% β^+ decay (635 keV positron energy) and is the most frequently used radionuclide in PET imaging, which is described in chapter 1.1.7.2. As described in chapter 1.1.4.1.1 fluorine-18 is produced by a cyclotron.[7] Two types of fluorination are used in the pharmaceutical field. The comparison is shown in Table 2 and described in chapter 1.1.5.1 and 1.1.5.2.

Table 2: Comparison of nucleophilic and electrophilic fluorination.[7]

	Nucleophilic fluorination	**Electrophilic fluorination**
Nuclear reaction	$^{18}O(p,n)^{18}F$	$^{18}O(p,n)^{18}F$
Target	$[^{18}O]H_2O$	$[^{18}O]O_2$
Fluorination agent	$[^{18}F]F^-$	$[^{18}F]F_2$
Molar activity (activity/mol)	100 GBq/µmol[7]	100 – 600 MBq/µmol[7]

1.1.5.1 NUCLEOPHILIC FLUORINATION

Nucleophilic fluorination was also used in the practical part of this master thesis. After the production of fluorine-18 by a cyclotron, the fluoride ions form hydrogen bonds with the surrounding water molecules and nucleophilic substitution is not working anymore. Azeotropic drying with acetonitrile and subsequent reaction in polar aprotic solvent is necessary to achieve the nucleophilic fluorination (Figure 5). The addition of a phase transfer catalyst, such as Krytofix 222, enhances the solubility and nucleophilicity of $[^{18}F]$fluoride ions. Once the drying is complete, the $[^{18}F]$fluoride ions can be used for nucleophilic substitution on an aliphatic position or for nucleophilic aromatic substitution on an aromatic molecule.[7]

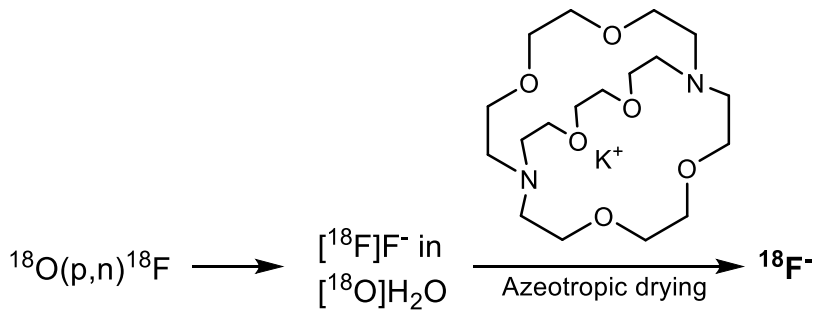

Figure 5: Production of fluoride-18 for nucleophilic fluorination.

1.1.5.2 ELECTROPHILIC FLUORINATION

For the production of the electrophilic $[^{18}F]F_2$ for an electrophilic fluorination a carrier molecule $[^{19}F]F_2$ is necessary to extract the radioactivity from the cyclotron target. The radioactive molecule can be used directly for the electrophilic fluorination. Due to the fact, that every ^{18}F-atom is bound to an ^{19}F-atom in a mixed $[^{18}F/^{19}F]F_2$ molecule, the maximum radiochemical yield is limited to 50%. Also, the regioselectivity is limited. It is possible to convert the $[^{18}F]F_2$ to a more selective fluorination agent like acetyl hypofluorite before labeling.[7]

1.1.6 THE CHEMISTRY OF GALLIUM AND THE RADIOCHEMISTRY OF GALLIUM-68

Gallium has the electron configuration $[Ar]3d^{10}4s^24p^1$ and exists in the metallic form and in two oxidation states, +1 and +3. Ga^{3+} with its three electrons in the outer shell is stable in aqueous solution and therefore interesting for *in vivo* experiments.[9] The small size and high charge density make it a strong Lewis acid forming stable complexes with strong Lewis bases with for example amino and oxy donors. Its main geometry is octahedral with six ligands, but also forms complexes with four and five ligands.[8–12] Ga^{3+} is highly dependent on pH values. In aqueous solution the trivalent cation is only stable under acidic conditions. Depending on temperature, Ga^{3+} forms insoluble $Ga(OH)_3$ and other species with low solubility between pH 3.5 and 7.5.[9,13] Those colloidal or pseudo-colloidal precipitates cannot form complexes anymore.[9] At pH > 7 stable tetracoordinate gallate ions $[Ga(OH)_4]^-$ are formed.[13] Under pH 4, $[Ga(H_2O)_6]^{3+}$ is the main species.[13]

Gallium-68 has a half-life of 67.71 min with 89% β^+ decay and 11% electron capture. The maximum positron energy is 1880 keV and it is produced by a $^{68}Ge/^{68}Ga$-generator (see chapter 1.1.4.2.1). With its properties and availability to label peptides and small molecules, it is used for clinical PET imaging.[8] Within 30 – 120 min, the used ^{68}Ga-chelator-peptide conjugates accumulate at the target site and clear rapidly from the blood.[13]

There are challenges that must be overcome when using gallium-68 for radiolabeling. A problem is the competing metal ions in the stationary phase of the generator, in this case titanium, that can reduce the labeling efficiency. High selectivity of the chelator to $[^{68}Ga]Ga^{3+}$ is necessary to prevent other metal ions from binding.[13] Radiolabeling of sensitive biomolecules sometimes require higher pH, which leads to the competing reactions obtaining the desired product plus gallium-colloid.[13] The *in vivo* stability is also an important factor to consider. The radiolabeled complex should be resistant to trans-chelation to transferrin. Due to the similar ionic radii of Fe^{3+} and Ga^{3+} the competing bindings to the two binding sites for threefold positively charged cations of transferrin could occur when synthesizing a receptor-targeted

radiotracer. Many chelators like the one in this thesis ($DATA^{5m}$) are in research and focus on current challenges.[13]

1.1.7 IMAGING TECHNIQUES

Tomographic techniques such as PET and SPECT, also combined with CT or MRI, are important imaging methods in nuclear medicine.[6] They set an important milestone to evaluate and investigate biological processes and physiological functions.[14] In this chapter, the principles of operation are described. A comparison of the techniques is shown in Table 3.

Table 3: Comparison of imaging techniques.[14]

	Spatial resolution	Sensitivity [mol/liter]	Advantages	Disadvantages	Principle
SPECT	1 – 2 mm	10^{-11} – 10^{-10}	No cyclotron needed, no tissue penetration limit	Low spatial resolution	Low energy γ-rays
PET	1 – 2 mm	10^{-12} – 10^{-11}	High sensitivity, whole-body images	High cost, cyclotron needed	High energy γ-rays
CT	50 – 200 µm	10^{-6}	High spatial resolution, fast measurement	Radiation	X-rays
MRI	25 – 100 µm	10^{-9} – 10^{-6}	High spatial resolution, no radiation	High cost, long measurement	Radio waves

1.1.7.1 SPECT - SINGLE PHOTON EMISSION COMPUTED TOMOGRAPHY

Nowadays, SPECT is usually built in gamma cameras. It is used for imaging of the brain, myocardial perfusion, skeletal and tumors.[15] In principle, low-energy γ-rays like in PET are detected, but radioisotopes for SPECT imaging only emit one photon. Those are for example iod-123 or technetium-99m. The γ-camera rotates around the body to obtain many images from different positions resulting in three-dimensional images. Due to the required collimator, the sensitivity of SPECT is not as high as in PET imaging.[14] The resolution of the image is better the lower the energy of the photon.[16]

1.1.7.2 PET - POSITRON EMISSION TOMOGRAPHY

The imaging with positron emission tomography uses indirectly produced high-energy γ-rays emitted of radionuclides like carbon-11, fluorine-18 or gallium-68.[14] It is mostly used for imaging of heart, lungs and brain.[16] Through the interaction of positrons and electrons (annihilation) two γ-rays with energies of

511 keV are set free moving in opposite directions.[14] Those are then detected simultaneously.[17] The patient is surrounded by multiple detectors typically built circular or hexagonal.[6] Photons are detected from different angles and through computer analysis three dimensional images are reconstructed. Due to the short half-lives of most radioisotopes used in PET, a cyclotron on-site is almost always needed with some exceptions like gallium-68.[14]

1.1.7.3 PET/SPECT-CT/MRI

The hybrid methods PET/SPECT images with CT/MRI are used for diagnostics such as the localization of cancer.[6] The multimodality imaging can help to obtain images of subjects registered in space and time.[18]

1.1.8 Design of radiopharmaceuticals

A radiopharmaceutical for diagnostics and therapy consists of three main components: The radionuclide, the linker and the targeting molecule (Figure 6). The radionuclide provides the radioactivity needed and is dependent on the application either in therapy or in diagnostics. The linker connects the radionuclide with the targeting molecule. In case of an organic radionuclide, the linker is a covalent bond. Metallic radionuclides are attached through bifunctional chelating agents, that form a stable complex. The targeting molecule, also called the vector molecule, can be a peptide, a protein, an antibody fragment or small inorganic or organic molecules. Necessary for the function as a targeting molecule are the properties like the specificity and selectivity for the target, which can be a receptor, transporter systems, enzymes and many more.[19]

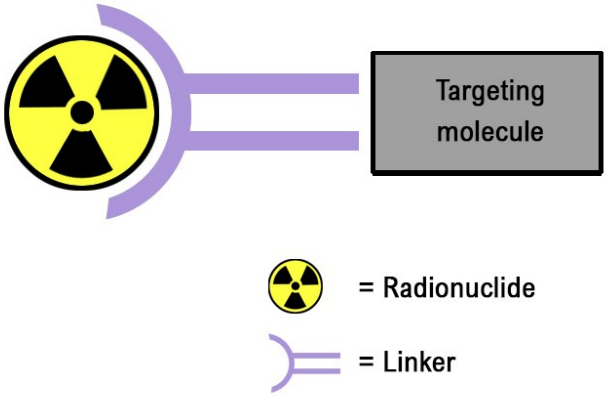

Figure 6: General design of a radiopharmaceutical.

1.1.9 Quality control of radiopharmaceuticals

For the administration of radiopharmaceuticals to human or animal specific parameters and limits must be met. Those are also shown in chapter 3.2.1.3.5 and chapter 3.2.2.3. The quality control includes measurements to ensure chemical, radiochemical, microbiological and radionuclidic purity.[6]

Physicochemical tests like the pH, osmolality and the purity are done right after the synthesis. The radiochemical purity is determined by HPLC and TLC / iTLC, whereat HPLC can determine the chemical purity *via* UV detector at the same time. The amount of solvent in the sample is measured by gas chromatography. Also, a γ-spectrum is recorded to determine the radionuclidic purity. Due to the short half-life of the radiopharmaceuticals, the sterility and endotoxin test is done after product release.[6]

1.2 FATTY ACID METABOLISM

Fatty acids are long carbohydrate chains with a carboxyl group at the end and are crucial for the energy metabolism in mammals. They are transported through the vascular and lymphatic system in form of triacylglycerols or as non-esterified (free) fatty acids. The main fatty acid binding protein with seven binding sites for fatty acids is albumin. The binding is necessary due to their low solubility in aqueous solution. After the transportation into the cells, they are β-oxidized. Energy is released in form of adenosine triphosphate and is the main energy source of the myocardium and skeletal muscle.[20–22]

1.2.1 RADIOTRACER

To investigate the fatty acid oxidation rate in the heart and skeletal muscle the sulfur atom containing ^{18}F-labeled tracer, 14-*(R,S)*-[^{18}F]fluoro-6-thia-heptadecanoic acid ([^{18}F]FTHA), is used amongst others. The PET-imaging with this radiotracer is a noninvasive technique for the investigation of β-oxidation to detect abnormalities in the myocardium and skeletal muscle.[21] It was assumed that [^{18}F]FTHA is metabolized mainly in the mitochondria in the heart. Around 89% of the radiolabeled tracer in the heart enter the mitochondria.[23] When [^{18}F]FTHA enters the skeletal muscle, it is mostly taken up by other cells and only around 36% move into the mitochondria.[23]

The synthesis of radiotracers for the fatty acid oxidation was investigated since many years and due to the increasing interest, transfer from manual to the automated synthesis was done. The automated production of [^{18}F]FTHA was performed by Savisto *et al*. with decay-corrected radiochemical yields of 13 ± 6.3% and by Pandey *et al*. of 16.9 ± 4.1%.[21,24] Savisto *et al.*'s approach was successful with radiochemical purities of over 95% and good stability at room temperature for a minimum of 4 hours. The appearance of an oxidized side product caused by radiolysis was avoided by the addition of ascorbic acid.[21] The synthesis by Pandey *et al*. gave different radiochemical purities when taking fractions with high (2.4 GBq/mL) and low (0.9 GBq/mL) radioactivity concentration. 10 min after radiosynthesis, radiochemical purity dropped lower than 93.5% and after 4 hours to 62.8% in the product of high radioactivity and to 86.7% after 4 hours in the one with low radioactivity concentration. Both were not pure enough for clinical use. The formation of a side product was investigated, and the relation between the side product and the sulfur atom was confirmed. In time the oxidation to sulfoxides increased. To

block radiation-induced instabilities, the addition of bovine serum albumin, human serum albumin, intralipid and ascorbic acid was tested but all approaches failed to give better radiochemical purities.[24]

By the comparison of the synthesis parameters in both studies, the starting radioactivity was much lower in the synthesis of Savisto *et al*. with 6 – 34 GBq compared to the one of Pandey *et al*. with 37 – 74 GBq. The radiation-induced side product was prevented in the synthesis with lower radioactivity (0.2 GBq/mL)[21], but could not be blocked after the synthesis of [^{18}F]FTHA with higher radioactivity like in the studies of Pandey *et al* (0.9 – 2.4 GBq/mL).[24]

Both studies were performed with automated synthesis modules specifically for ^{18}F-radiotracers and the synthesis time was around 1 hour.[21,24]

1.3 FIBROBLAST ACTIVATION PROTEIN (FAP)

FAP is a type II transmembrane serine protease and belongs to the prolyl peptidase family. It has most similarities with dipeptidyl peptidase IV (DPPIV) sharing 52 to 70% of its amino sequence identity.[25,26] Dipeptidyl peptidases cleave the *N*-terminal Pro-X peptide bond (X = any amino acid except hydroxyproline or proline) by hydrolysis. DPPIV and FAP have dipeptidyl peptidase enzymatic activity, but only FAP has endopeptidase activity. FAP is overexpressed in tissue remodeling sites like fibrosis, chronic inflammation, arthritis, or tumors and is not detectable in most healthy tissue. It is only expressed in activated fibroblasts, what makes it an interesting target for imaging and therapeutic techniques with the help of radionuclides. The activated fibroblasts in tumors are called cancer associated fibroblasts and are most likely responsible for the regulation in tumor biology and the composition of the matrix.[25–28]

1.3.1 FAP-SPECIFIC ENZYME INHIBITORS

FAP inhibitors block the enzymatic activity by binding the active site of FAP.[29] A promising example as a FAP-specific enzyme inhibitor is the UAMC-1110 (Figure 7).[28] It has a high selectivity and low nanomolar affinity towards FAP but not dipeptidyl peptidase and endopeptidase prolyl oligopeptidase.[29] It is also under examination as a therapeutic radiopharmaceutical. Later, a radiotracer called FAPI-02 was developed by Lindner and Loktev *et al*.,[27] that consists of DOTA as a chelator and piperazine as a linker to the FAP inhibitor (Figure 8). The [^{68}Ga]Ga-FAPI-02 showed a high tumor and a low normal tissue uptake and also fast clearance from the blood. Various other inhibitors were developed with structural varieties like the FAPI-04, FAPI-05 and FAPI-46 (Figure 9). They all have the structure of UAMC-1110 as inhibitor in common (Figure 9). The low FAP-affinity and high tumor uptake made them to promising radiopharmaceuticals for imaging and theranostics.[28]

Further development of radiotracers using bifunctional DOTA and DATA^{5m} chelators with squaramide as linker (Figure 9; **d** and **e**) have shown good stability and also high affinity to FAP. Macrocyclic chelators like DOTA form thermodynamically stable and kinetically inert complexes with gallium-68.[30] The synthesis of the precursor is easy and convenient due to the selectivity of squaric acid (SA) for primary amines. No protecting group is necessary and the coupling works under mild conditions and is pH-controlled.[28] The DATA^{5m} chelator was radiolabeled under mild conditions with gallium-68 versus the DOTA chelator required high temperatures for the complexation with gallium-68 and lutetium-177.[28] Stability studies were performed by Moon *et al*.[28] with good results above 95% over a period of 2 hours in both cases, [^{68}Ga]Ga-DATA^{5m}.SA.FAPi and [^{68}Ga]Ga-DOTA.SA.FAPi. The first one was determined in ethanol, human serum and saline 0.9% and the second one in phosphate buffered saline, human serum and saline 0.9%.[28] [^{68}Ga]Ga-DOTA.SA.FAPi was also tested against trans-chelation and trans-metalation (EDTA, DTPA, Cu, Mg, Ca and Fe).[28] Clinical studies for DATA^{5m}.SA.FAPi by Moon *et al*.[29] showed tracer uptake in focal nodular hyperplasia.[29]

Recently, Moon *et al.* developed a novel FAP inhibitor with AAZTA as chelator (Figure 10). The radiolabeling was successful under mild conditions and the product AAZTA^{5}.SA.FAPi showed excellent stability over a period of 2 hours in human serum, ethanol and saline with values over 99.9%.[29]

Studies showed, that after synthesis of ^{68}Ga-labeled compounds with high specific activities, the formation of insoluble ^{68}Ga-species in PET-imaging results in decreased ratios of target to background due to the uptake in the spleen, liver and bone marrow.[31,32] The use of solid-phase extraction to purify the product is most commonly used in clinical practice. It is fast, convenient and cheap.[31]

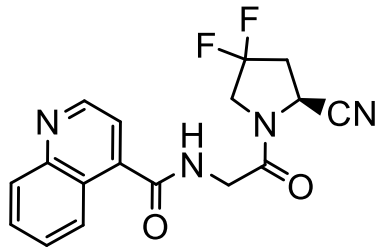

Figure 7: UAMC1110.

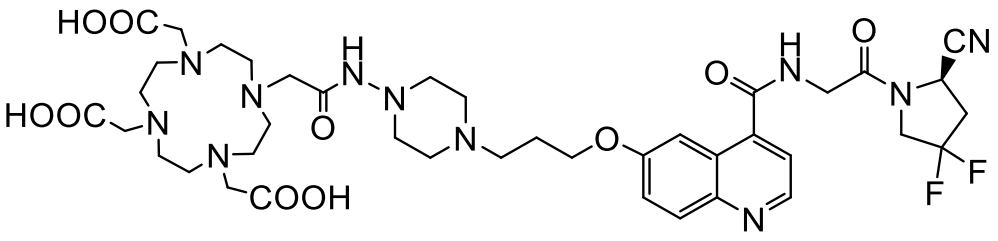

Figure 8: FAPI-02.

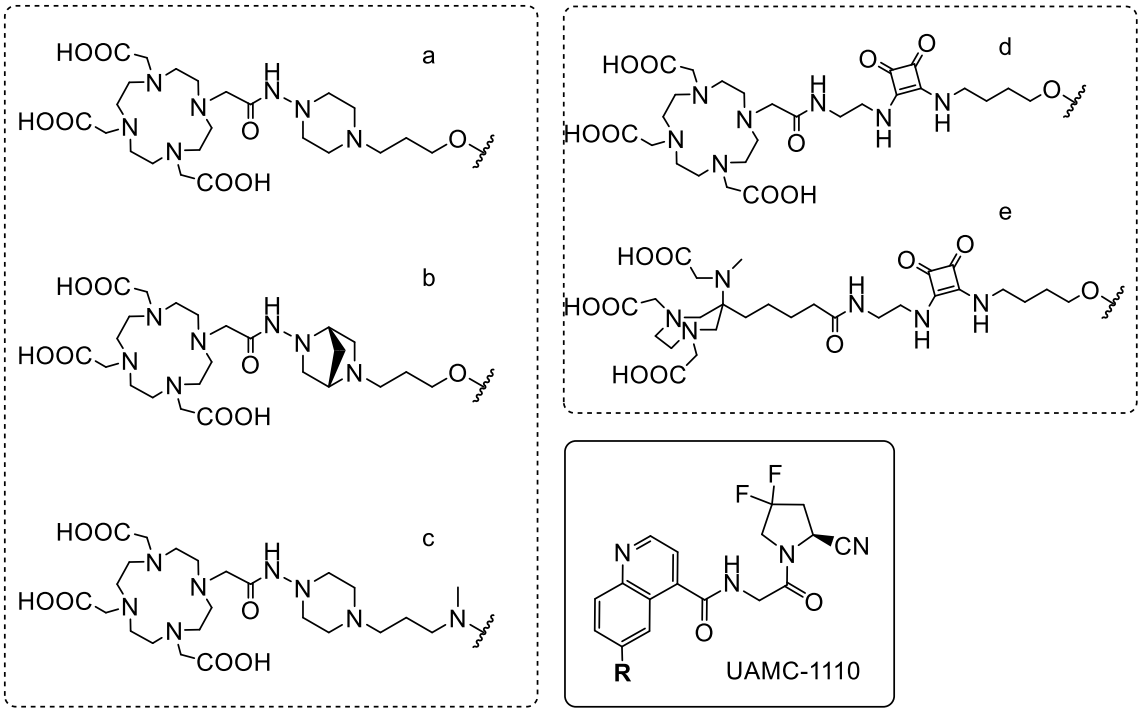

Figure 9: Structures of different chelators and linker of the FAP inhibitor UAMC-1110. **a**: FAPI-04; **b**: FAPI-21; **c**: FAPI-46; **d**: DOTA.SA.FAPi; **e**: DATA^{5m}.SA.FAPi.

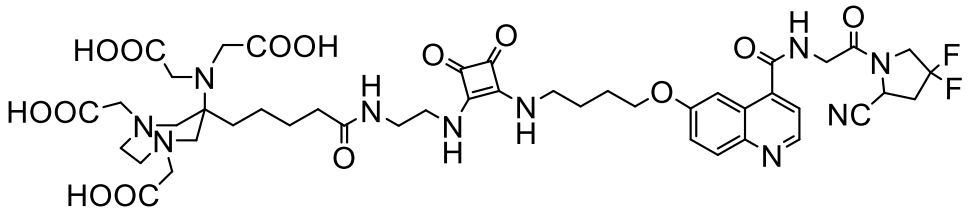

Figure 10: AAZTA^{5}.SA.FAPi.

2 RESULTS AND DISCUSSION

2.1 AIM OF THIS THESIS

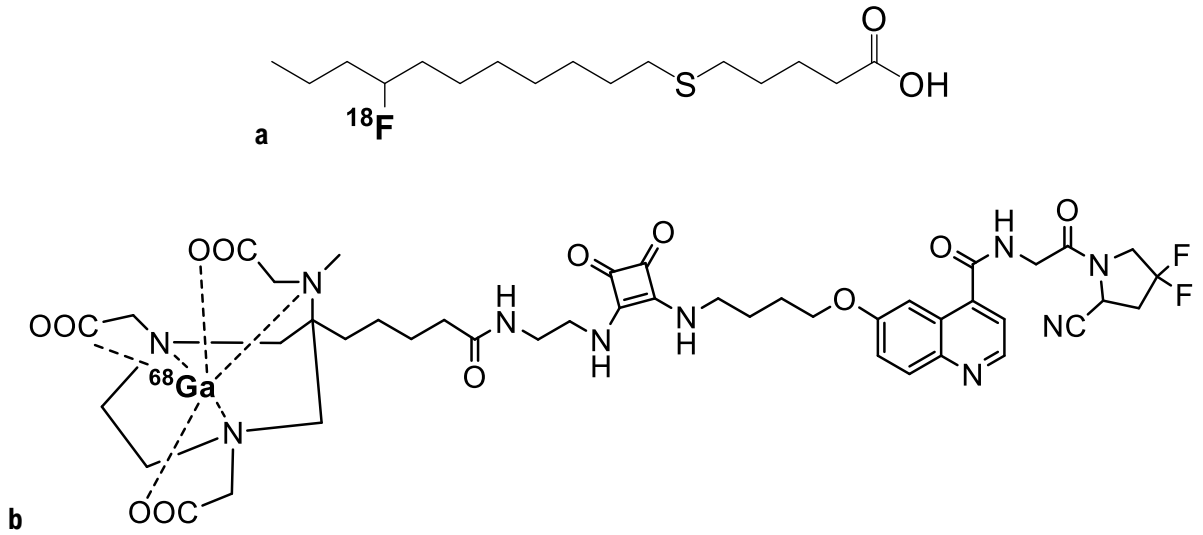

Figure 11: Radiotracer. a: [^{18}F]FTHA; b: [^{68}Ga]Ga-DATA^{5m}.SA.FAPi.

The aim of this thesis was the radiolabeling of two different molecules: The DATA^{5m}.SA.FAPi is radiolabeled with gallium-68 (Figure 11; **b**) and 14-*(R,S)*-fluoro-6-thia-heptadecanoic acid (FTHA) with fluorine-18 (Figure 11; **a**). The objective was the successful synthesis for *in vivo* studies and the determination of the stability over time. Variation of different parameters and reaction conditions should be varied and further, the synthesis of [^{18}F]FTHA transferred to an automated synthesis module. With the help of radio-HPLC and radio-TLC compounds **a** and **b** should be characterized. Furthermore, the stability of both radiolabeled tracers should be determined. The two radiotracers should in the future be used in human trials and integrated in the routine application in hospitals.

2.2 RADIOLABELING OF BENZYL-14-*(R,S)*-TOSYLOXY-6-THIAHEPTADECANOATE

The radiolabeling consists of two reaction steps: The nucleophilic substitution and the hydrolysis (Figure 12). To obtain the desired labeled fatty acid the carbonate group got protonated with an acid.

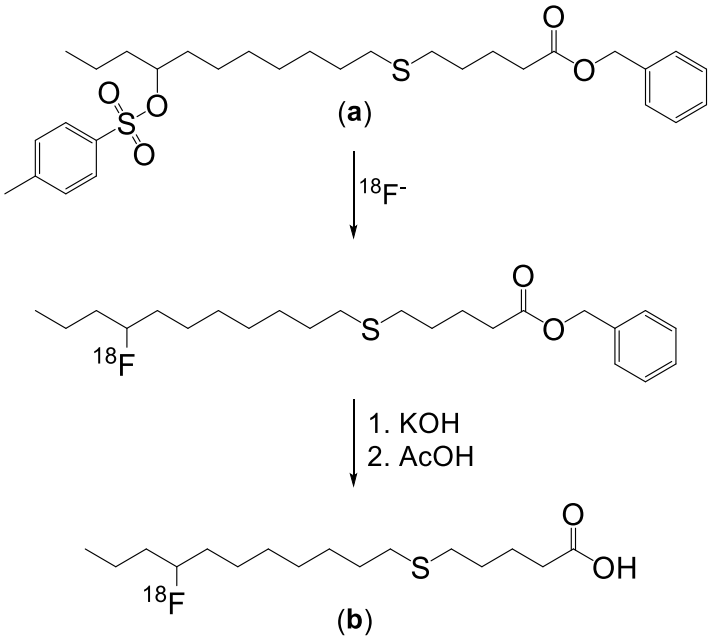

Figure 12: General reaction scheme; **a**: precursor (Benzyl-14-*(R,S)*-tosyloxy-6-thiaheptadecanoate); **b**: product (14-*(R,S)*-[^{18}F]fluoro-6-thia-heptadecanoic acid).

The first step of the radiolabeling was the S_N2 reaction to exchange the leaving group p-toluenesulfonate with fluorine-18 (shown in Figure 13).

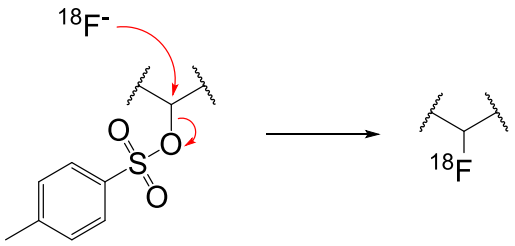

Figure 13: Nucleophilic substitution (S_N2).

The next step was the separation of the alcohol protecting group benzyl *via* basic hydrolysis with potassium hydroxide followed by the neutralization with acetic acid (shown in Figure 14).

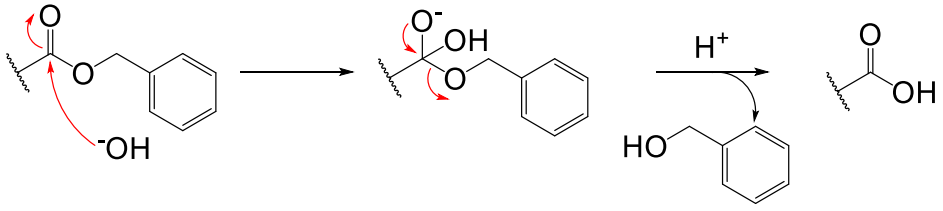

Figure 14: Hydrolysis and neutralization.

2.3 Determination of the linear calibration curve

For the calculation of remaining precursor and calculation of amount of non-radioactive product respectively, a linear calibration curve was determined shown in Diagram 1.

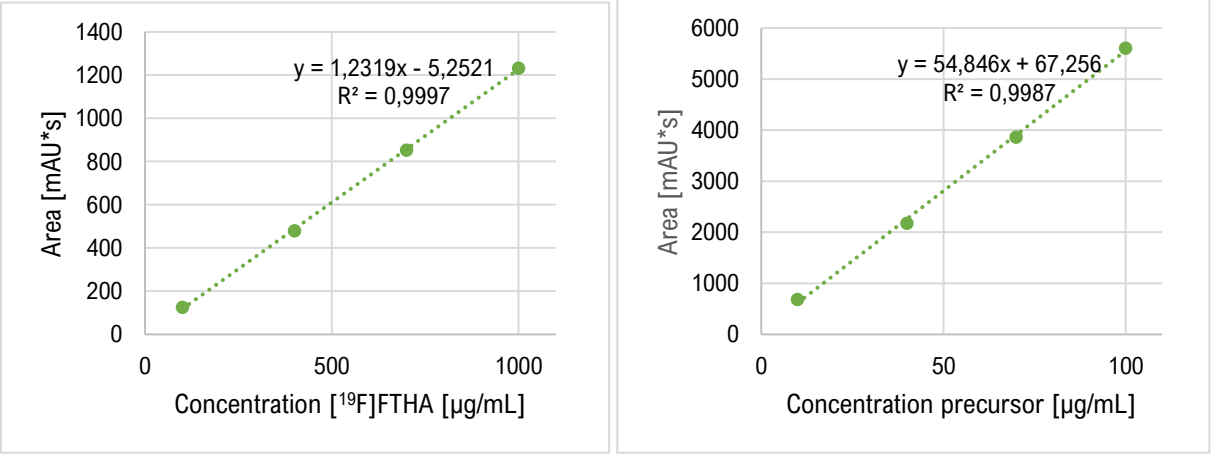

Diagram 1: Left: Linear calibration curve for amount of standard; right: Linear calibration curve for amount of precursor.

2.4 Manual synthesis of [18F]FTHA

2.4.1 General procedure

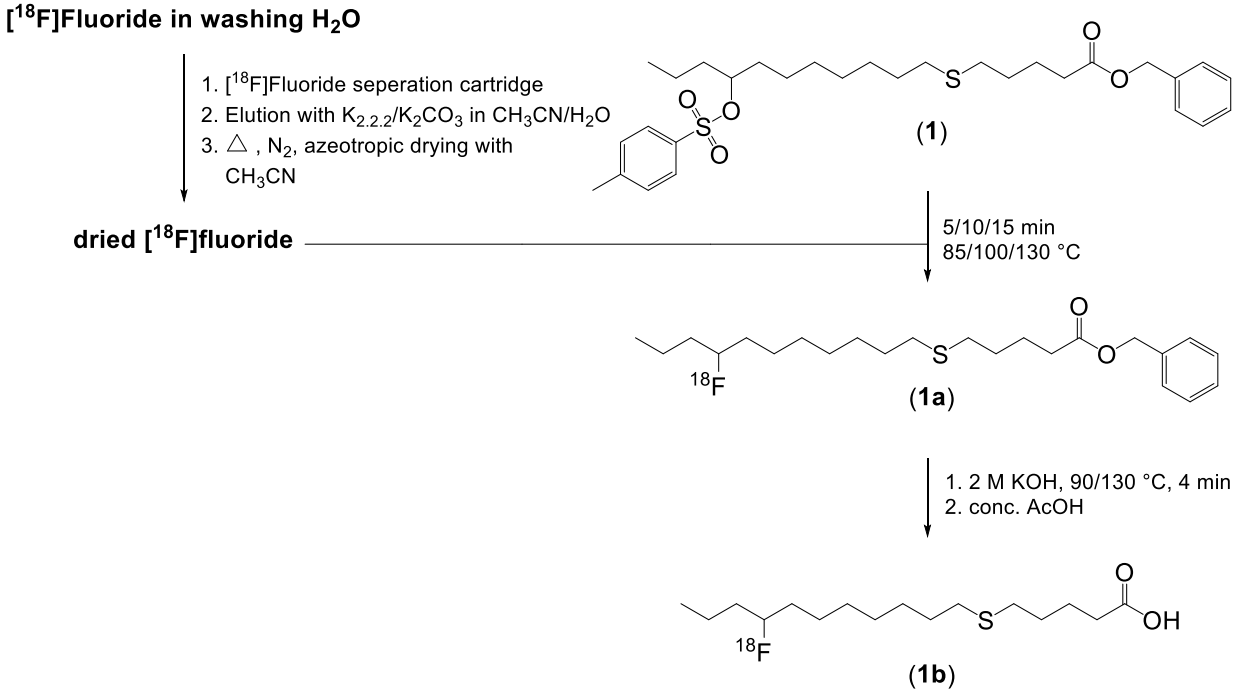

Figure 15: Manual synthesis of [18F]FTHA.

A scheme of the manual synthesis is shown in Figure 15. After drying of the [18F]fluoride ions, it was reacted with the precursor (**1**) and the protecting group removed to obtain the desired product (**1b**). The phase-transfer catalyst Kryptofix 222 was used to facilitate the reaction and increase the reactivity of the

[^{18}F]fluoride ion.[33] Nucleophilic substitution was performed in polar aprotic solvent, that leads to S_N2 reactions. Due to the solvation of the cation the reactivity of the fluoride ions is increased leading to an easier substitution of the tosylate leaving group. A protic solvent would interact with the fluoride ion and result in a lower nucleophilicity. The formation of the [^{18}F]fluoro ester (**1a**) was checked by radio-TLC (Figure 16). Two peaks were visible on the TLC plate, the free [^{18}F]fluoride ions with Rf values around 0.0 and the [^{18}F]fluoro ester with Rf values between 0.8 – 1.0. After radiolabeling, basic ester hydrolysis was performed with potassium hydroxide to remove the benzyl protecting group. The protonation to obtain product (**1b**) was the last step (radiochemical incorporation rates shown in Table 4). The characterization was performed with radio-HPLC (Figure 17). Radio-TLC characterization of the final product was not reliable with immense peak variation when comparing to the results of the radio-HPLC.

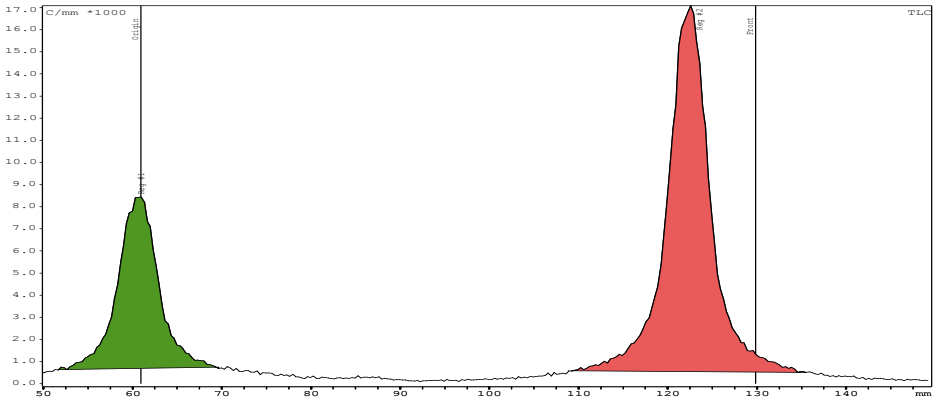

Figure 16: Radio-TLC characterization with peaks for [^{18}F]fluoride ion and [^{18}F]fluoro ester (**1a**).

2.4.2 Optimization and results

In Table 4 the results of the manual syntheses of [^{18}F]FTHA (described in chapter 3.2.1.2.2 - 3.2.1.2.5) are shown. The product was characterized by radio-HPLC with retention times of free [^{18}F]fluoride ions around 2 min and [^{18}F]FTHA around 4 min 25 sec.

Table 4: Radiochemical purities of the different synthesis methods characterized by radio-HPLC.

Synthesis method	n	Average radiochemical incorporation rate (RCI) [%]
1	10	52 ± 24
2	2	9 ± 5
3	2	15 ± 10
4	2	30 ± 15

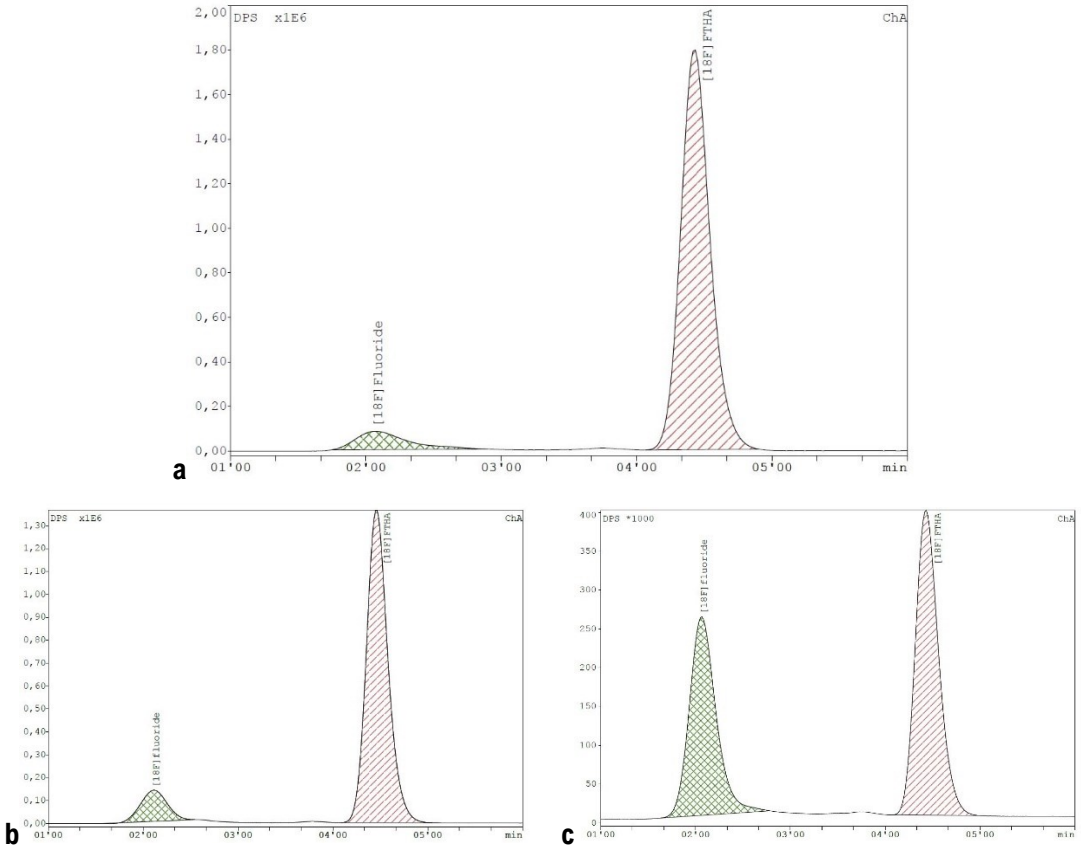

Figure 17: Analytical HPLC results of manual syntheses.

Different reaction parameters were tested to improve conversion to [^{18}F]FTHA (shown in Table 13). The results show enhanced radiochemical purity with increasing temperature. Longer reaction times could increase the purity at lower temperature but synthesis method 2 with 85 °C reaction temperature was not effective and showed very low radiolabeling. Synthesis method 1 was performed with 2 and 4 mg/mL precursor, whereby the higher concentration led to better radiochemical purities. Most automated syntheses were therefore conducted with higher precursor concentrations (4 mg/mL). Due to not constant conditions and unpredictable problems, like a broken heater or septum, results varied. Also, the manual syntheses were performed without preparative HPLC to see the ratio of the radiolabeled product compared to the amount of unreacted [^{18}F]fluoride (Table 4).

2.5 AUTOMATED MODULE SYNTHESIS OF [^{18}F]FTHA

2.5.1 GENERAL PROCEDURE

The general procedure of the automated synthesis is shown in Figure 18 and was adapted from Savisto *et al*.[21] The [^{18}F]fluoride ions were produced by a cyclotron, dried *via* azeotropic drying and reacted with the precursor. Additionally to the procedure in chapter 2.4.1, the product was formulated for clinical use. Therefore, after HPLC purification, the synthesized radiotracer [^{18}F]FTHA was pushed through a solid

phase cartridge, washed with *Aqua ad inj.* and then eluted with ethanol. The final product was diluted with physiological saline solution and quality control was done.

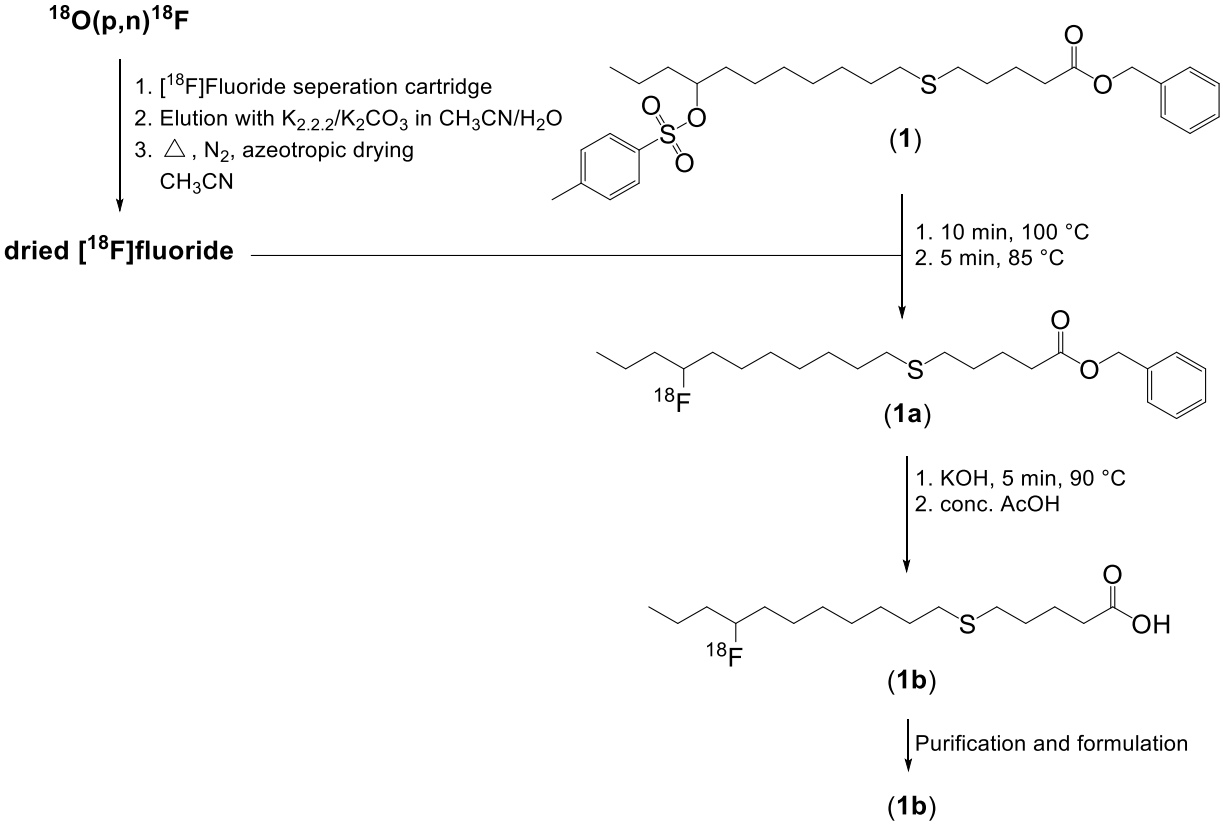

Figure 18: Automated synthesis of [^{18}F]FTHA.

In Table 5 all parameter variations of the different syntheses on the automated module are shown. All syntheses were performed as described in chapters 3.2.1.3.

Table 5: Variation of automated synthesis parameter.

Parameter	**Variation**
Precursor concentration [mg/mL]	3, 4, 5
Number of azeotropic dryings	2, 3
Sterile filter	Yes, No
Amount of ethanol in V5 [mL]	0.5 – 1.5
Amount of [^{18}F]fluoride [GBq]	25 – 55

2.5.2 OPTIMIZATION AND RESULTS

For the optimization of the synthesis different parameters were varied and compared (Table 5). First, the manual synthesis was transferred onto the automated synthesis module, second the optimization of the parameters was done and results compared (Table 7).

First, the focus of the synthesis was on the general feasibility of the procedure. After successful installation, the optimization focused on the application in (pre)clinical studies whereby the amount of radioactivity in 100 µL product was important. By comparing the efficiency of the synthesis with different concentrations, the decay-corrected (to the end of bombardment) radiochemical yield of selected syntheses (Table 6) are compared. The most successful syntheses are performed with 4 mg/mL precursor concentration, which is also chosen for the end protocol. For application on animals or human, the amount of ethanol must not exceed 10%. Table 7 shows the different amounts tested and the radioactivity in 100 µL product. The elution with 0.8 mL ethanol was successful with lost radioactivity values on the cartridge of 13 ± 3% *versus* 16 ± 9% with 0.7 mL ethanol. The azeotropic drying was performed either two or three times. By the comparison of decay-corrected yields, 10 ± 1% (n = 2) were obtained with two and 13 ± 4% (n = 5) with three azeotropic dryings (1 and 1.5 mL ethanol respectively used for the elution). The program was set to three drying steps after evaluation. Radiochemical yields are also dependent on the initial radioactivity. The final synthesis program was tested with 44 and 55 GBq of initial activity, respectively. Decay-corrected yields of the lower starting activity were 11 ± 5% (n = 3) and 8 ± 1% (n = 3) for the higher starting radioactivity. To conclude, more radioactivity is lost in the synthesis module with higher initial activities and depending on the desired end formulation, the starting radioactivity can be adapted.

Table 6: Comparison of precursor concentrations with obtained yields.

n	Precursor concentration [mg/mL]	Average decay-corrected radiochemical yield [%]	Amount ethanol for elution [mL]
3	3	7 ± 2	1.5
5	4	12 ± 2	1.5
3	5	12 ± 5	0.8

Table 7: Comparison of various automated syntheses.

Initial radioactivity [GBq]	Amount precursor [mg/mL]	Amount ethanol [mL]	Decay-corrected radiochemical yield [%]	MBq in 100 µL	Sterile filter
17.2	3	1.5	9	6.7	
27.6	3	1.5	8	7.7	
28.5	3	1.5	5	4.8	
28.7	4	1.5	13	11.6	
27.8	4	1.5	12	11.3	
27.8	4	1.5	12	11.5	
27.6	4	1.5	13	12.9	
27.8	4	1.5	9	9.8	
42.4	4	0.5	9	45.8	
28.0	4	1	10	17.2	
38.5	4	1	20	43.0	
40.5	4	0.7	15	49.6	
52.7	4	0.7	8	35.3	
41.5	4	0.8	13	38.8	
55.7	4	0.8	9	37.3	
27.8	5	0.8	17	32.1	
27.7	5	0.8	7	13.8	
27.7	5	0.8	11	23.0	
54.2	4	0.8	9	35.0	✓
44.7	4 – 8	0.8	16	46.8	✓
43.9	4	0.8	9	30.6	✓
44.1	4	0.8	16	51.0	✓
43.7	4	0.8	6	18.5	✓
54.8	4	0.8	7	31.8	✓

The characterization with radio-HPLC and radio-TLC always showed high radiochemical purities exceeding 95% (Figure 19). All measured properties needed for quality control met the limits that are shown in Table 16. The application of a sterile filter is optional, in both cases the quality control was successful with losses of 9 ± 1% on the filter. The decay-corrected (to the end of bombardment) radiochemical yield of [^{18}F]FTHA was 10 ± 3% for the optimized synthesis parameters with the use of a sterile filter (Table 8).

Table 8: Synthesis results for optimized method. EOS = end of synthesis; RCY = radiochemical yield, RCP = radiochemical purity.

Total	Failed	RCP [%]	Activity EOS [GBq]	Decay-corrected RCY [%]
7	0	99.5 ± 0.3	2.8 ± 0.8	9.9 ± 3.4

For better results, a dedicated ^{18}F-module could be used[21,24] to avoid evaporations into the lines during the azeotropic drying and fast wear of the module. The automated module used in this thesis is originally for ^{11}C syntheses that are without heavy heating. For the azeotropic drying high temperatures are necessary, but it could not be set to the 130 °C which resulted in best yields in the manual syntheses (Table 4). The temperatures were set like described in chapter 3.2.1.3. Also, the peak collection from the preparative HPLC needed to be done manually and due to connection problems between module and computer, some syntheses failed. Enhanced nucleophilic fluorination can also be tested with additional phase transfer catalyst Kryptofix 222 to accelerate the azeotropic drying in acetonitrile and increase reactivity of [^{18}F]F$^-$. The positively charged counter ion potassium complexes Kryptofix 222 and prevents the formation of [^{18}F]KF.[34,35] Another important aspect to consider is the reactivity of the chosen leaving group: Cl < Br < I < 4-methylbenzenesulfonate (tosylate) ~ methanesulfonate < trifluoromethanesulfonate. The precursor purchased in this thesis contains tosylate as leaving group, which could be exchanged with trifluoromethanesulfonate for better substitution results.

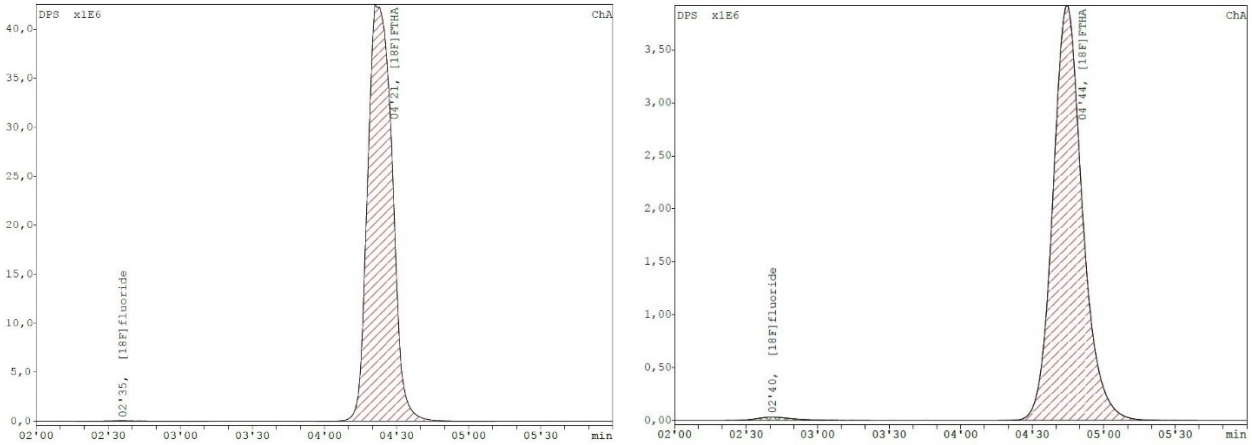

Figure 19: Analytical radio-HPLC characterization.

For routine production an automated synthesis module is preferable compared to manual syntheses and has the advantages of reliability, safety and reproducibility. Time and heating can be readjusted again when using a ^{18}F-module.

2.5.3 STABILITY TESTS

The stability of [^{18}F]FTHA was determined right after the synthesis and after approximately 1, 2, 3 and 4 hours. Results are shown in Diagram 2. In Figure 20 radio-HPLC results support the increasing decomposition to free [^{18}F]fluoride ions but there is no peak for oxidized products like described by Pandey *et al*.[24] The radioactivity per mL is lower than in the studies of Pandey *et al.* which could explain the better stability of [^{18}F]FTHA. Figure 21 shows an example of radio-TLC characterization. Within

4 hours, the TLC characterization didn't show any additional peaks and was stable. The radiotracer shows high stability at room temperature with radiochemical purities still over 97% 4 hours after synthesis.

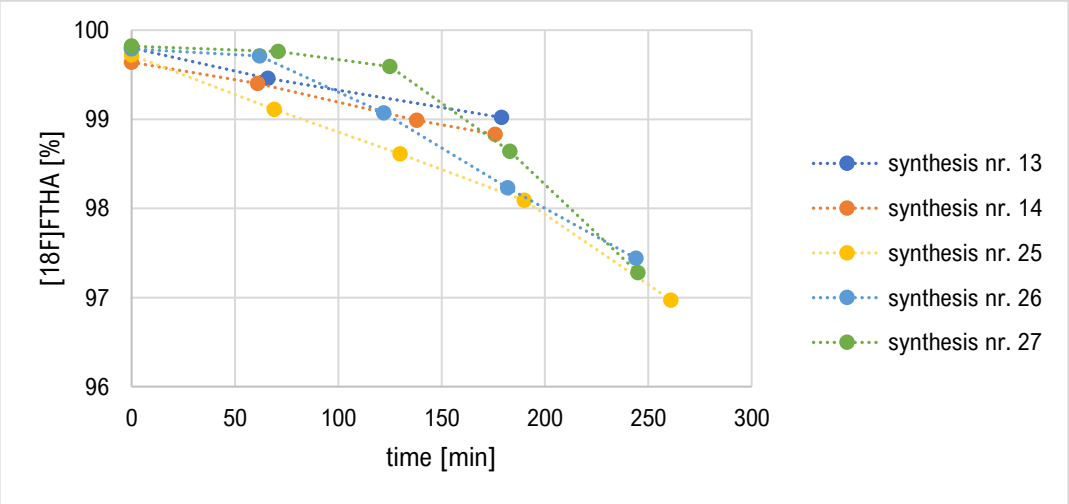

Diagram 2: Stability of [^{18}F]FTHA.

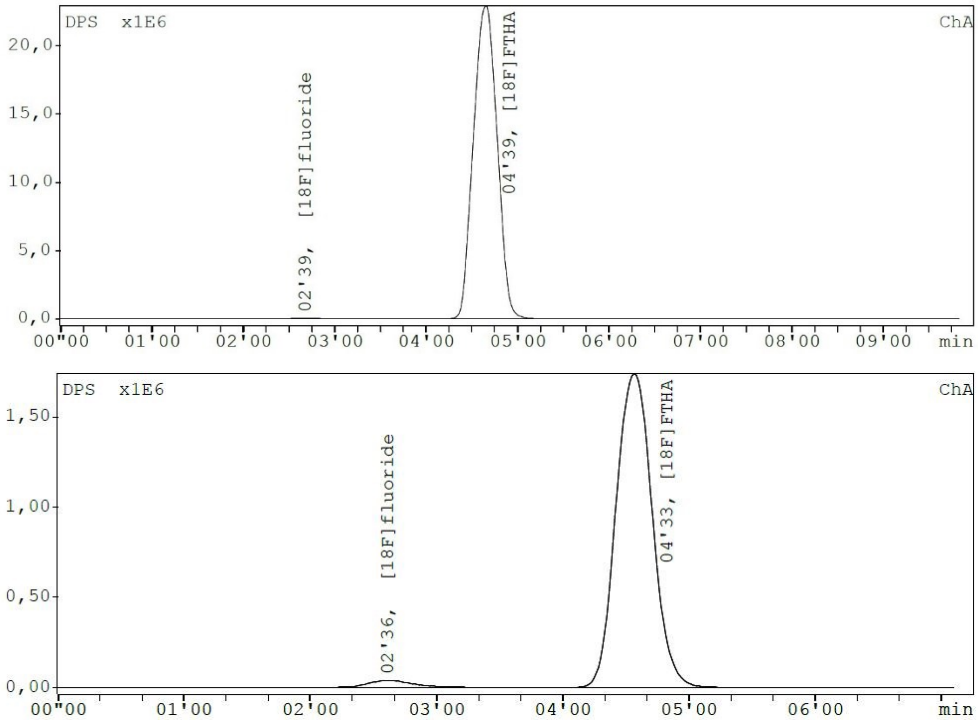

Figure 20: Radio-HPLC characterization of [^{18}F]FTHA. Top: Right after synthesis; bottom: 4 h after synthesis.

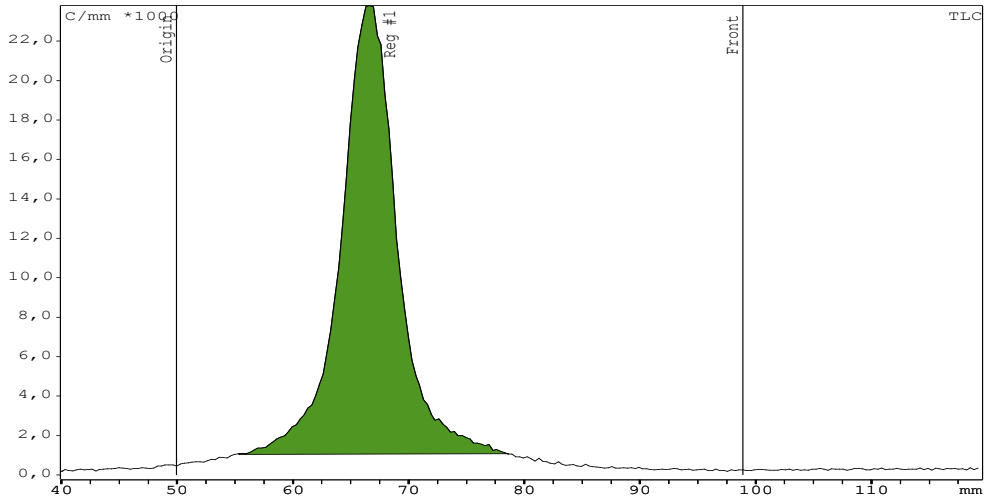

Figure 21: Radio-TLC characterization of [^{18}F]FTHA right after release.

Plasma stability tests are important to predict product stability problems in *in vivo* studies. Besides the formation of undesired radio-metabolites, unstable compounds could have rapid clearance and could result in the failure of studies.[36] Results for the plasma stability test are shown in Diagram 3. Timepoint 0 of the plasma stability test is not the end of the synthesis but the start of the test. [^{18}F]FTHA is most stable in human serum, which is also shown in Figure 23. The reference, which is the radiotracer without plasma and serum respectively, and the mouse plasma is almost equally stable with a small impurity of < 1% shown in Figure 22 and Figure 24. The impurity is less lipophilic than [^{18}F]FTHA and could be an oxidized side product like Pandey *et al*. suggested.[24] Stability tests of the radiotracer at room temperature didn't show any side products or impurities other than [^{18}F]fluoride ions.

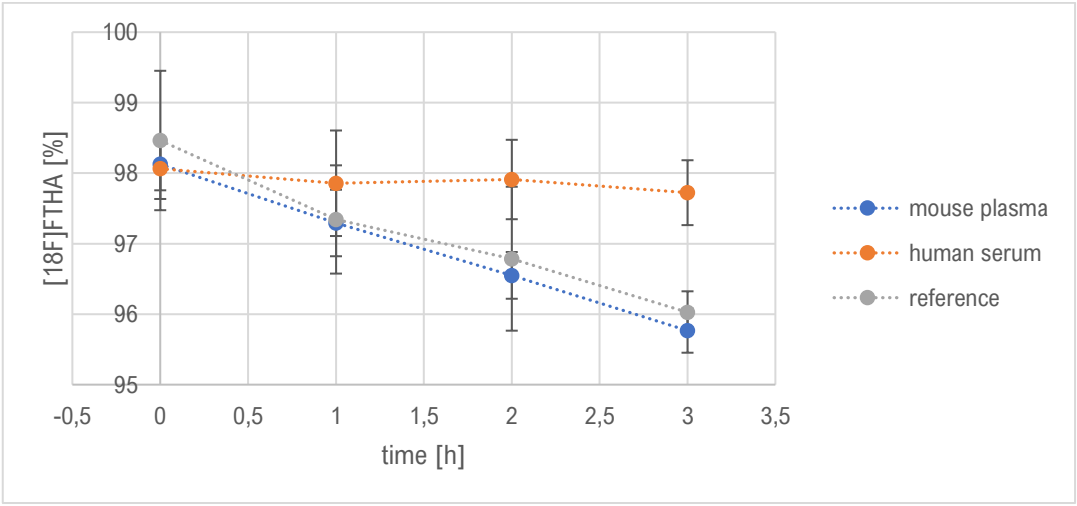

Diagram 3: Stability in mouse plasma and human serum of [^{18}F]FTHA.

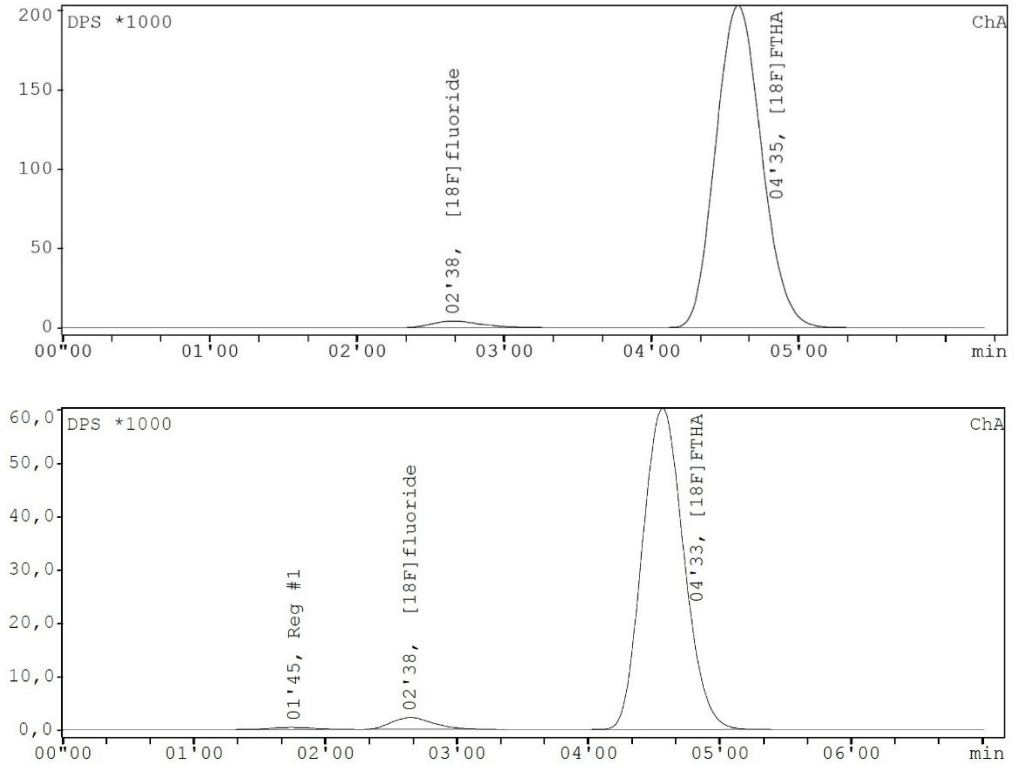

Figure 22: Radio-HPLC characterization of the reference. Top: right after synthesis; bottom: 3 h after synthesis.

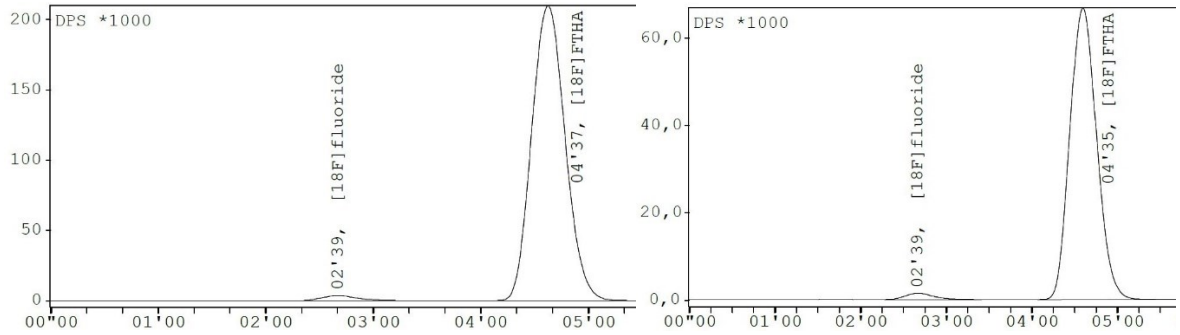

Figure 23: Radio HPLC characterization of [^{18}F]FTHA incubated with human serum at 37 °C. Left: right after synthesis; right: 3 h after synthesis.

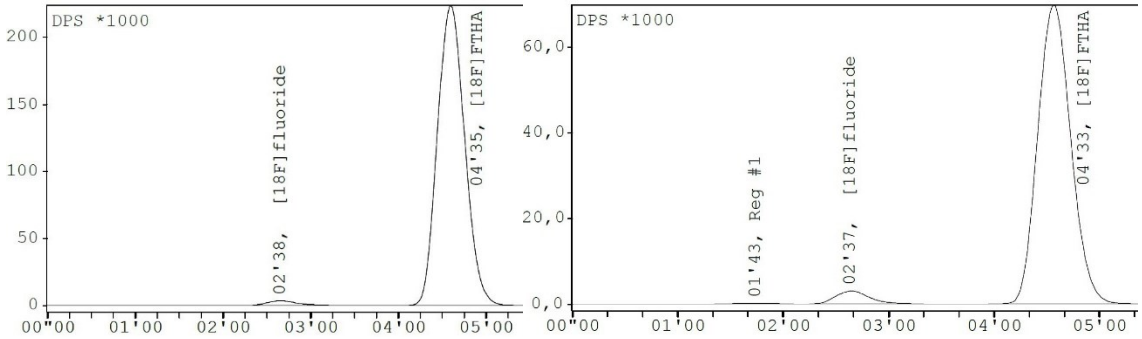

Figure 24: Radio HPLC characterization of [^{18}F]FTHA incubated with mouse plasma at 37 °C. Left: right after synthesis; right: 3 h after synthesis.

2.5.4 STUDIES

The radiotracer was tested *in vitro* on cells and *in vivo* on mice and rats. In this chapter the studies are shortly summarized.

[^{18}F]FTHA was tested on myocardial cells of the cell line H9C2 with promising results. The uptake of the synthesized radiotracer is significantly higher than the one of [^{18}F]FDG. However, the studies on this have not yet been completed.

Animal studies were performed multiple times with mice and rats. Static and dynamic distribution scans were performed on PET/MRI and PET/CT devices. An example picture of a PET/MRI scan, that was acquired by Ing. Usevalad Ustsinau MSc. during the project "Tracking Nutrient Metabolism and Cellular Partitioning by Multimodal Molecular Imaging" in the Preclinical Laboratory at the Medical University of Vienna, is shown in Figure 25.

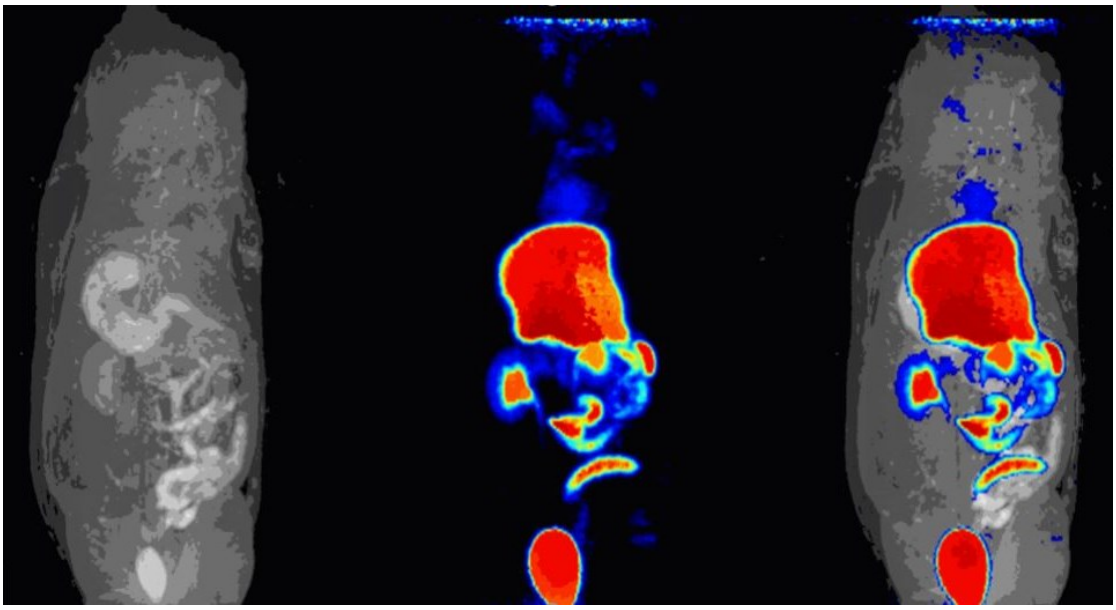

Figure 25: PET/MRI scan of rat injected with [^{18}F]FTHA. Visible organs: brain, heart, liver, kidneys, intestines and bladder.

2.6 RADIOLABELING OF DATA^{5M}.SA.FAPI

2.6.1 GENERAL PROCEDURE

The general procedure was adapted from the protocol sent by Prof. Rösch (Johannes Gutenberg Universität Mainz, Germany). For the radiolabeling, the precursor of [^{68}Ga]Ga-DATA^{5m}.SA.FAPi was reacted with gallium-68 and formulated for animal studies. Gallium-68 forms a chelate-complex with DATA^{5m} (Figure 26, (**2a**)).

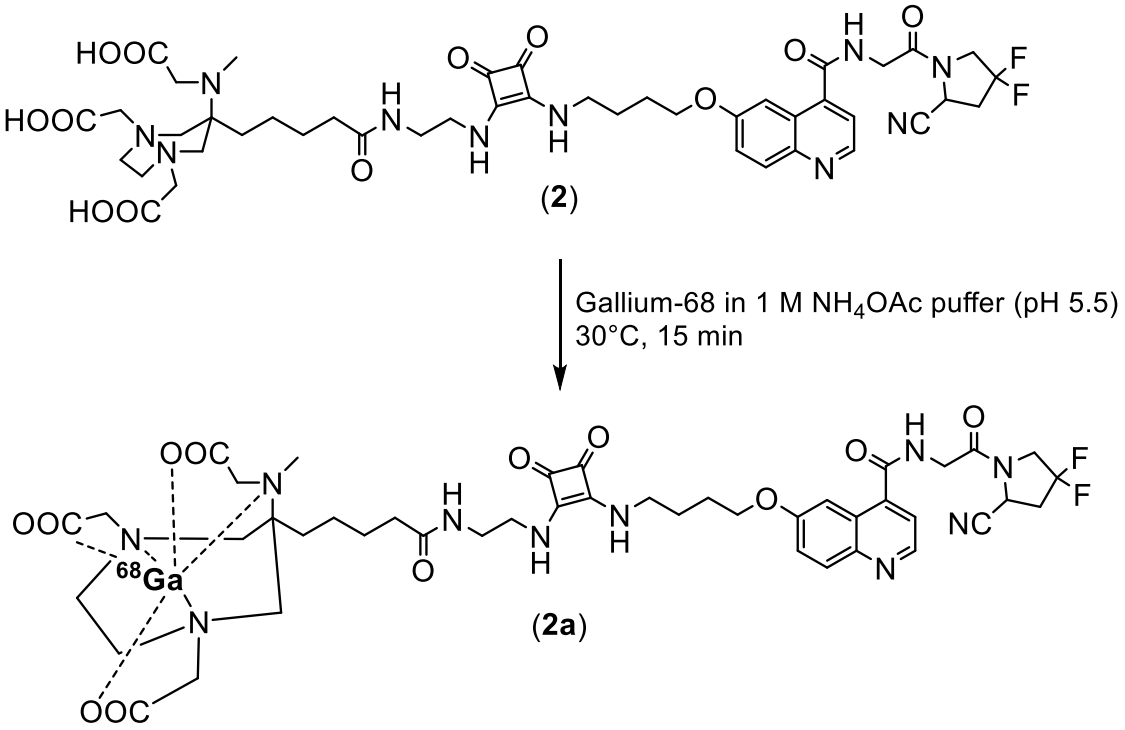

Figure 26: Synthesis of [^{68}Ga]Ga-DATA^{5m}.SA.FAPi.

2.6.2 Optimization and results

The focus of this part of the practical work lied on the successful radiolabeling with good radiochemical purities for studies. Results of the radiolabeling are shown in Table 9. The amounts of syntheses were limited to the amount of precursor delivered by the group of Prof. Rösch. Two generators were used for the synthesis. The maximum amount of produced radioactivity varied. One generator could produce up to 400 MBq and the other one up to 1200 MBq

Table 9: Results of the radiolabeling to obtain [^{68}Ga]Ga-DATA^{5m}.SA.FAPi.

n	Amount precursor [nmol]	Added radioactivity [MBq]	Average RCP (HPLC) [%]	Average RCP (iTLC) [%]
10	20	190 – 382	98.2 ± 1.2	97.2 ± 2.0
2	20	993 – 1000	96.0 ± 0.5	95.3 ± 0.9
1	25	1196	92.9	96.6
1	30	1200	92.2	96.4
1	42	980	97.0	97.9

The different parameters used for the radiolabeling are shown in Table 10. Results (Table 9) showed the more radioactivity used the less radiochemical purity for the same amount of precursor. Further radiolabeling studies are necessary to obtain the minimum precursor amount for larger amounts of radioactivity. The radiochemical purity was determined by radio-iTLC (Figure 27) and by radio-HPLC

(Figure 28). Radio-iTLC was first done with two different mobile phases, whereby the one with sodium citrate didn't give any qualitative results and showed only one peak for the colloid and the product together. The one with ammonium acetate showed ^{68}Ga-colloid with R_f values of 0 and the product with R_f values of 1. Amounts of free not reacted gallium-68 (R_t = 0.9 – 1.1) and product (R_t = 3.5 – 3.6 min) were determined by radio-HPLC analysis.

In chapter 3.2.2.3 limits for the quality control are shown. For the evaluation of the right pH and osmolality, different amounts of 1 M ammonium acetate buffer for the reaction and phosphate buffer or saline solution for the formulation were used (Table 10).

Table 10: Variation of the parameters.

Parameter	**Variation**
Precursor amount [nmol]	20 – 42
Amount of radioactivity [MBq]	190 – 1200
1 M NH_4OAc buffer (pH 5.5) [µL]	150, 300
Formulation liquids	0.9% NaCl, 125 mM Phosphate buffer
125 mM Phosphate buffer; [v%] of the entire mixture	50, 41, 33

Right after the synthesis the product was mostly pure enough for the animal studies, but clinical trials on humans would need further purification with a SepPak C-18 cartridge, where the product and the gallium-colloid get stuck. Afterwards, the elution of [^{68}Ga]Ga-DATA^{5m}.SA.FAPi with ethanol, further evaporation of the solvent and formulation with saline solution 0.9% is suggested by the group of Prof. Rösch.

2.6.3 STABILITY TESTS

The stability of [^{68}Ga]Ga-DATA^{5m}.SA.FAPi was determined right after synthesis, after 1, 2 and 3 hours by radio-HPLC and radio-iTLC (Figure 27, Figure 28). Diagram 4 shows different syntheses of [^{68}Ga]Ga-DATA^{5m}.SA.FAPi. Synthesis FAPi_17/18 were not stable with a starting radiochemical purity of 93% and a final radiochemical purity of 84 and 85% respectively. When comparing these results with the other syntheses, it is assumed, that the higher the radiochemical purity at the end of the synthesis, the slower the decomposition in time. For further research, it is necessary to focus on the stability. The higher the decomposition, the worse the target to background ratio in clinical PET imaging due to the higher accumulation of free [^{68}Ga]Ga^{3+} on other sites and less targeted imaging.

By looking at the comparison of the stability determined by radio-HPLC and radio-iTLC in Diagram 5, it can be assumed that almost only free [^{68}Ga]Ga^{3+} increases in time and that the amount of ^{68}Ga-colloid is almost constant.

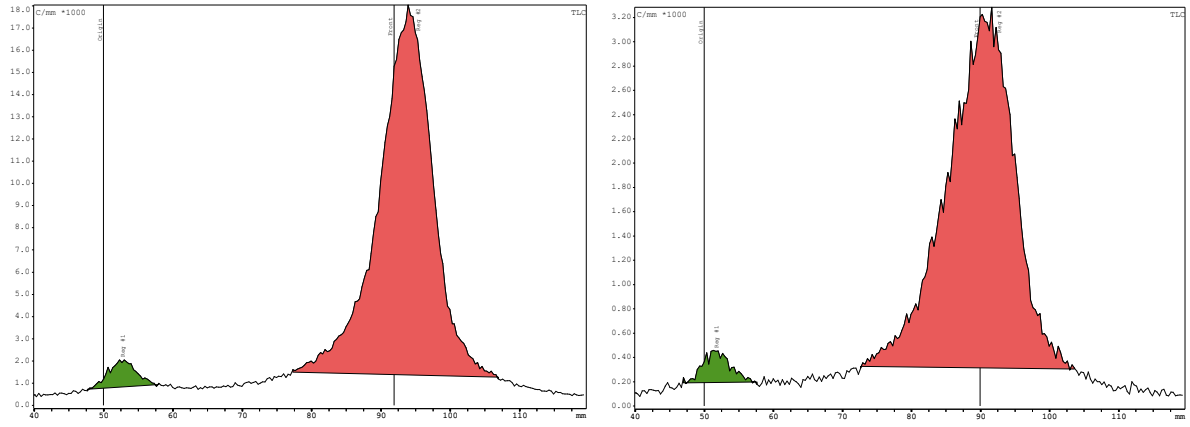

Figure 27: [^{68}Ga]Ga-DATA^{5m}.SA.FAPi determined by radio-iTLC. Left: Right after synthesis; right: 3 h after synthesis.

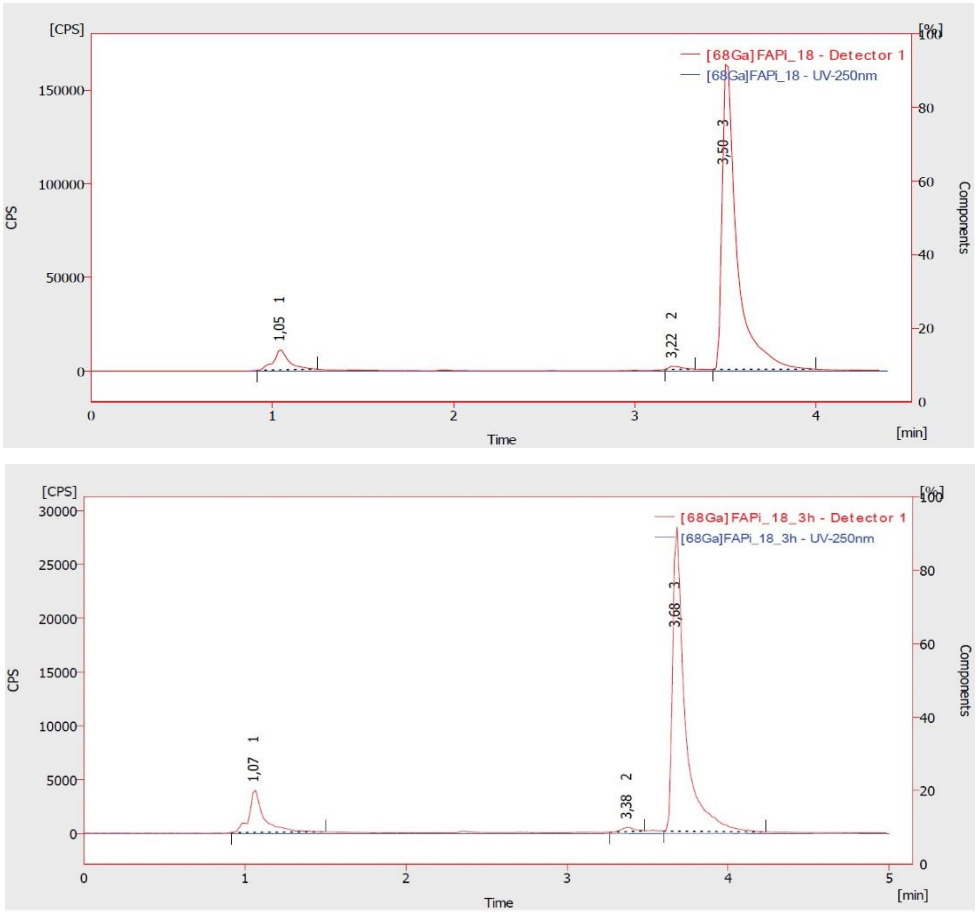

Figure 28: [^{68}Ga]Ga-DATA^{5m}.SA.FAPi determined by radio-HPLC. Top: Right after synthesis; bottom: 3 h after synthesis.

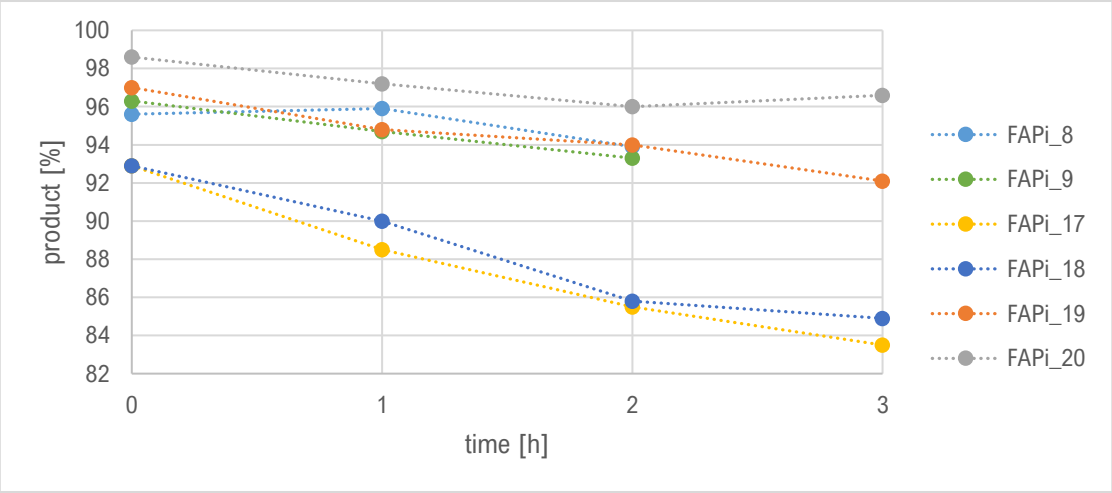

Diagram 4: Stability of [^{68}Ga]Ga-DATA^{5m}.SA.FAPi.

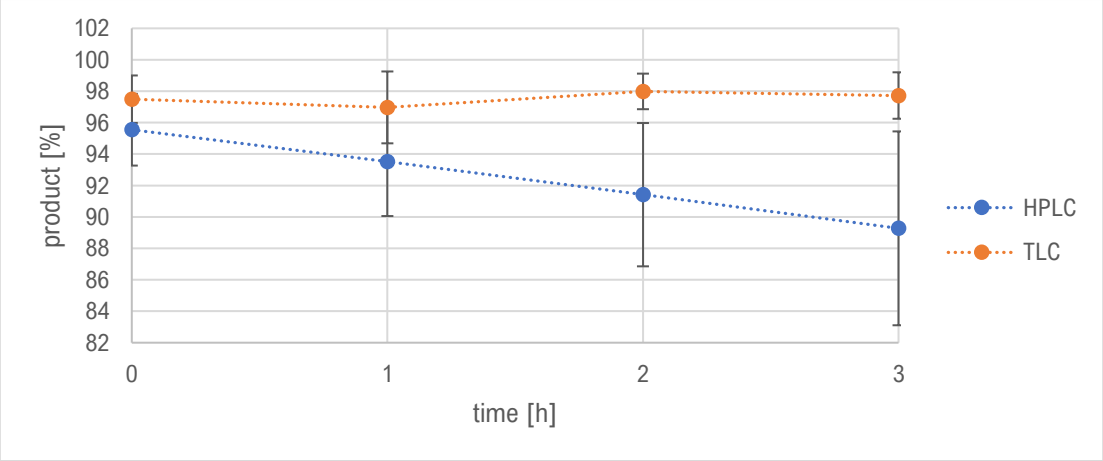

Diagram 5: Comparison of the stability of [^{68}Ga]Ga-DATA^{5M}.SA.FAPi determined by radio-HPLC and radio-iTLC. The mean value is plotted.

2.6.4 STUDIES

Animal studies were performed several times with [^{68}Ga]Ga-DATA^{5m}.SA.FAPi on mice. A PET/CT was used for the imaging. An example of a PET/CT scan of a mouse, that was acquired at the Medical University of Vienna, is shown in Figure 29.

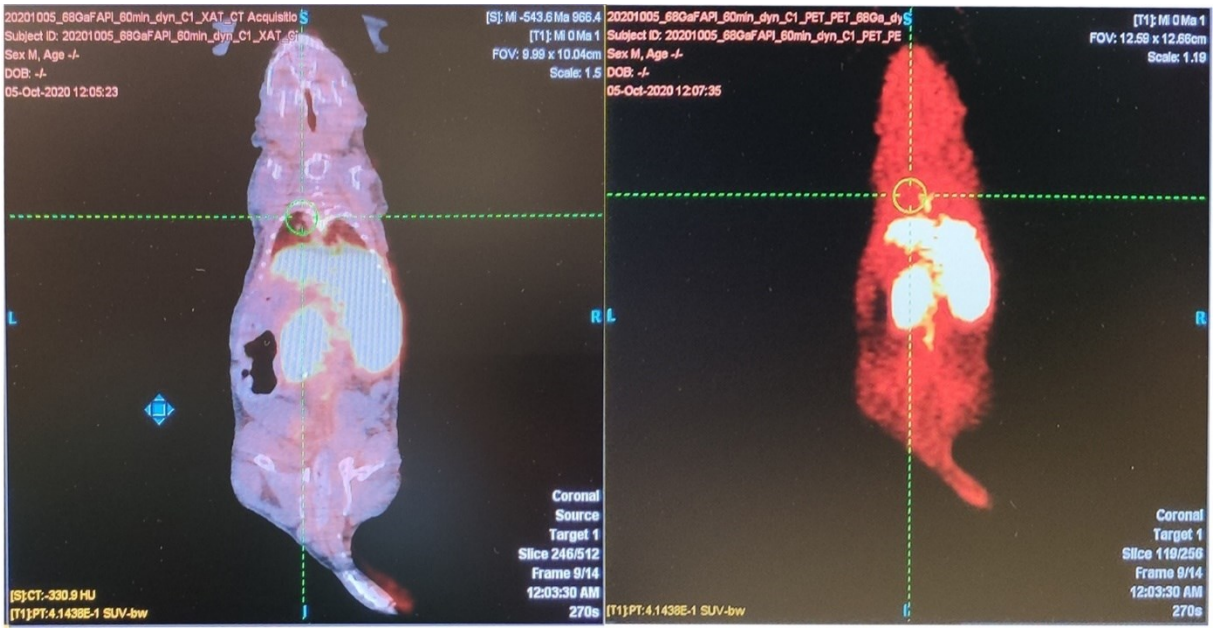

Figure 29: PET/CT scan of mouse injected with [^{68}Ga]Ga-DATA^{5m}.SA.FAPi.

3 EXPERIMENTAL PART

In this chapter the practical part and the analytical data are presented.

3.1 MATERIALS AND INSTRUMENTATIONS

All used chemicals were already on stock and purchased from Sigma Aldrich, Merck and VWR except the precursor of [^{68}Ga]Ga-DATA^{5m}.SA.FAPi that was given by Prof. Rösch. They were not further purified before usage. Gas bottles were purchased from Messer.

The used chemicals and machines are listed in Table 11 and Table 12 and described in chapter 3.1.1 and chapter 3.1.2.

Table 11: List of used chemicals.

Chemical	Product number	Company
Acetic acid	27225	Sigma-Aldrich
Acetone	20066	VWR Chemicals
Acetonitrile	34851	Sigma-Aldrich
Ammonium acetate	101116	Merck
L-Ascorbic acid	A5960	Sigma-Aldrich
Benzyl-14-*(R,S)*-tosyloxy-6-thiaheptadecanoate	2850	ABX
Ethanol	100986	Merck
Kryptofix® 222	810647	Merck
Methanol	34860	Sigma-Aldrich
Sodium chloride 9 mg/mL		B. Braun
Potassium carbonate	791776	Sigma-Aldrich
Potassium hydroxide	105032	Merck
Sodium acetate trihydrate	71188	Sigma-Aldrich
Sodium citrate dihydrate	W302600	Sigma-Aldrich
Sodium dihydrogen phosphate	106346	Merck
di-Sodium hydrogen phosphate	106580	Merck
TFA	T6508	Sigma-Aldrich
TraceSELECT® water	95305	Sigma-Aldrich
14-*(R,S)*-[^{18}F]Fluoro-6-thia-heptadecanoic acid	2860	ABX

Table 12: List of devices.

Device	Series	Company
Centrifuge	Universal 30 RF	Hettich
Heater / magnetic stirrer	Yellow line MST basic	IKA®
HPLC syringes	SYR 50 µL	Hamilton®
Micro analysis scale	Cubis® Individual	Sartorius
Milli-Q®	Direct 8	Merck
Needles	Microlance™ 3 Sterican®	BD B.Braun
pH-indicator strips	pH-Fix 2.0 – 9.0	Macherey-Nagel
Pipettes	Reference, Reference 2, Research plus	Eppendorf
Plastic needles	Micro Pin®	B-Braun
Product vials	8590.0011W DRN 4370	ABX Curium™
Syringes	Injekt®	B.Braun
ThermoMixer	ThermoMixer C	Eppendorf
Temperature sensor	Yellow line TC 1	IKA®
Vortex	L24	Labinco

3.1.1 [^{18}F]FTHA

The irradiation was performed with a GE PETtrace™ cyclotron (GE Medical Systems) and a control system (GE Medical Systems COROS OP15).

All manual syntheses were performed in a lead hood (5vm Pb, Type B). The washing water from the cyclotron line with fluoride ions was transported in a 5 mL Wheaton vial with a lead shielding and also in a lead box. For the automated syntheses a former ^{11}C-methylation PET-synthesizer (formerly Nuclear Interface®, now General Electric Medical Systems, Uppsala, Sweden) was used and the [^{18}F]fluoride ions were transferred into a 2.5 mL Wheaton vial. The liquid nitrogen was filled in a Dewar vessel (KGW-Isotherm, Type 22AL, 3 liter) for transportation. For the purification a filter unit (Sep-Pak® Plus Light C18) and the yellow sterile filter (Millex®GV Filter Unit 0,22 µm from Merck) were used.

The quality control was carried out with pH stripes (Macherey-Nagel; pH-Fix 2.0 – 9.0), an osmometer (WESCOR VAPRO® 5600 Osmometer), the Kryptofix test (Celltech K222-TAA and the solution S from Celltech), the GC, the HPLC and the TLC.

The analytical HPLC measurements were performed with the VWR Hitachi assembled with the Chromaster 5160 pump, the 5310 Column Ovan, the 5410 UV detector (set to 230 nm) and the Raytest Gabi radiodetector. The connected column was the Gemini® 10 µm C18 110Å (Phenomenex;

250x10 mm) and the mobile phase 90:10:0.4 = MeOH:H_2O:AcOH. All results were integrated with the software GinaStar.

The preparative HPLC measurements were performed with the HPLC column Gemini® 10 µm C18 110Å (Phenomenex; 250x10mm) using a mobile phase with the ratio of 850:150:4:2(v/v/v) MeOH/H_2O/AcOH/Ascorbic acid.

For the evaluation of the TLCs the Raytest Gita Star with the Raytest Gamma BGO-V-detector was used and the integration was done with the software TLC Control (Gita) and Gina Star TLC Ramona S. The thin-layer chromatography for the final product was performed on the TLC Silica gel 60 RP-18 $F_{254}S$ from Merck (mobile phase: 100:10:0.4 MeOH/H_2O/CH_3COOH (v/v/v)). The [^{18}F]fluoro ester formation during the manual syntheses was tracked on the TLC Silica 60 F_{254} from Merck (mobile phase: 3:1 Hexane/EtOAc).

The gas chromatograms were recorded by the Bruker 430-GC with an autoinjector (Bruker CP-8410) and interpreted with the Software Galaxie Chromatography Data System (Varian).

3.1.2 [^{68}Ga]Ga-DATA^{5M}.SA.FAPi

Gallium-68 was produced by the radionuclide generator Galli Ad 0,74 – 1,85 GBq (IRE Elit Belgium).

The analytical HPLC measurements were performed with the VWR Hitachi assembled with the Chromaster 5160 pump, the 5310 Column Ovan, the 5410 UV detector (set to 220 nm) and the Raytest Gabi radio detector. The connected column was the Chromolith® Performance RP-18e 100 – 4.6 mm. The method for the measurements was set with a linear gradient (0.5 – 10 min, 5 – 95% CH_3CN (+0.1% TFA) / 95 – 5% H_2O (+ 0.1% TFA); 2 mL/min flow).

For the evaluation of the iTLCs the Raytest Gita Star with the Raytest Gamma BGO-V-detector was used and the integration was done with the software TLC Control (Gita) and Gina Star TLC Ramona S. The thin-layer chromatography was performed on the iTLC-SG from Agilent Technologies (mobile phase: 1:1 1 M NH_4OAc/MeOH pH 7.4; 0.1 M Sodium citrate·3H_2O pH 5).

3.2 Methods

3.2.1 [^{18}F]FTHA

3.2.1.1 Preparation of the analytical and preparative HPLC

For the later characterization of the final product [^{18}F]FTHA, the non-radioactive reference standard 14-*(R,S)*-fluoro-6-thiaheptadecanoic acid dissolved in EtOH (100 µg/mL, 400 µg/mL, 700 µg/mL and 1 mg/mL) was measured by the analytical HPLC. The precursor of [^{18}F]FTHA, Benzyl-14-*(R,S)*-tosyloxy-6-thiaheptadecanoate dissolved in acetonitrile (10 µg/mL, 40 µg/mL, 70 µg/mL and 100 µg/mL) was also

measured by the analytical HPLC. The mobile phase was a mix of methanol, Milli-Q® water and acetic acid in the ratio 90:10:0.4 (v/v/v). A linear calibration curve was generated (shown in Diagram 1) for calculation of the amounts of precursor and non-radioactive product in the final formulation.

3.2.1.2 MANUAL SYNTHESIS OF [^{18}F]FTHA

The first step of the manual synthesis of [^{18}F]FTHA was the azeotropic drying of the [^{18}F]fluoride ions and then the conversion to the product with variation of parameters shown in Table 13. It was characterized by radio-HPLC and radio-TLC, whereas the results of the radio-TLC varied too much for consideration.

Table 13: Different methods of the manual syntheses of [^{18}F]FTHA.

Synthesis	Precursor concentration [mg/mL]	Reaction time [min]	Reaction temperature [°C]	Hydrolysis temperature [°C]
Method 1	2, 4	15	130	130
Method 2	2	15	85	90
Method 3	2	5	100	90
Method 4	2	10	100	90

3.2.1.2.1 AZEOTROPIC DRYING

The [^{18}F]fluoride was collected from the washing water of the target line from the cyclotron. It was pushed through a ^{18}F-separation cartridge (45 mg PS-HCO_3^-) and the [^{18}F]F^- was eluted with a solution of Kryptofix 222 and potassium carbonate dissolved in CH_3CN/H_2O (500 µL of a 1 mL 80/20 CH_3CN/water (v/v) solution with 20 mg K_{222}, 4.5 mg K_2CO_3). The mixture was heated under a constant stream of nitrogen for 15 min at 120 °C. Acetonitrile (3 x 300 µL) was added during these 15 minutes.

3.2.1.2.2 SYNTHESIS METHOD 1

The precursor dissolved in acetonitrile (40 µL, 2 mg/mL; 4 mg/mL) was added to the dried [^{18}F]fluoride in acetonitrile (40 µL). The reaction mixture was stirred for 15 minutes at 130 °C and subsequently cooled with ice. The formation of [^{18}F]fluoro ester was checked by radio-TLC. KOH (24 µL, 2 M) was added and the solution stirred for 4 minutes at 130 °C. The mixture was cooled with ice, concentrated acetic acid (2.4 µL) was added and vortexed. The product was characterized by radio-HPLC and radio-TLC. Radiochemical incorporation rate: 52 ± 24%. R_f = 0.4 - 0.6 (100:10:0.4 MeOH/H_2O/CH_3COOH); R_t = 4m25s (90:10:0.4 MeOH/H_2O/AcOH).

3.2.1.2.3 SYNTHESIS METHOD 2

The precursor dissolved in acetonitrile (40 µL, 2 mg/mL) was added to the dried [^{18}F]fluoride in acetonitrile (40 µL). The reaction mixture was stirred for 15 minutes at 85 °C and subsequently cooled with ice. The formation of [^{18}F]fluoro ester was checked by radio-TLC. KOH (24 µL, 2 M) was added and the solution stirred for 4 minutes at 90 °C. The mixture was cooled with ice, concentrated acetic acid (2.4 µL) was added and vortexed. The product was characterized by radio-HPLC. Radiochemical incorporation rate: 9 ± 5%. R_t = 4m26s (90:10:0.4 MeOH/H_2O/AcOH).

3.2.1.2.4 SYNTHESIS METHOD 3

The precursor dissolved in acetonitrile (40 µL, 2 mg/mL) was added to the dried [^{18}F]fluoride in acetonitrile (40 µL). The reaction mixture was stirred for 5 minutes at 100 °C and then the heater was turned off and the mixture was stirred for another 10 min where the temperature dropped to 80 °C. Subsequently it was cooled with ice. The formation of [^{18}F]fluoro ester was checked by radio-TLC. KOH (24 µL, 2 M) was added and the solution stirred for 4 minutes at 90 °C. The mixture was cooled with ice, concentrated acetic acid (2.4 µL) was added and vortexed. The product was characterized by radio-HPLC. Radiochemical incorporation rate: 15 ± 10%. R_t = 4m26s (90:10:0.4 MeOH/H_2O/AcOH).

3.2.1.2.5 SYNTHESIS METHOD 4

The precursor dissolved in acetonitrile (40 µL, 2 mg/mL) was added to the dried [^{18}F]fluoride in acetonitrile (40 µL). The reaction mixture was stirred for 10 minutes at 100 °C and then let cool down for 5 minutes (minimum: 90 °C). Subsequently it was cooled with ice. The formation of [^{18}F]fluoro ester was checked by radio-TLC. KOH (24 µL, 2 M) was added and the solution stirred for 4 minutes at 90 °C. The mixture was cooled with ice, concentrated acetic acid (2.4 µL) was added and vortexed. The product was characterized by radio-HPLC and radio-TLC. Radiochemical incorporation rate: 29 ± 15%. R_t = 4m26s (90:10:0.4 MeOH/H_2O/AcOH).

3.2.1.3 AUTOMATED MODULE SYNTHESIS OF [^{18}F]FTHA

The first step was the cleaning and preparation of the module before each use. Afterwards, the production of the [^{18}F]F$^-$ was done using the cyclotron of the AKH Vienna. The next step was the synthesis with the automated synthesis module including the azeotropic drying and the formation and purification of the final product.

3.2.1.3.1 SCHEME AND DESCRIPTION OF THE MODULE

In Figure 30 the schematic buildup of the module used is shown. All symbols and vials are described in Table 14.

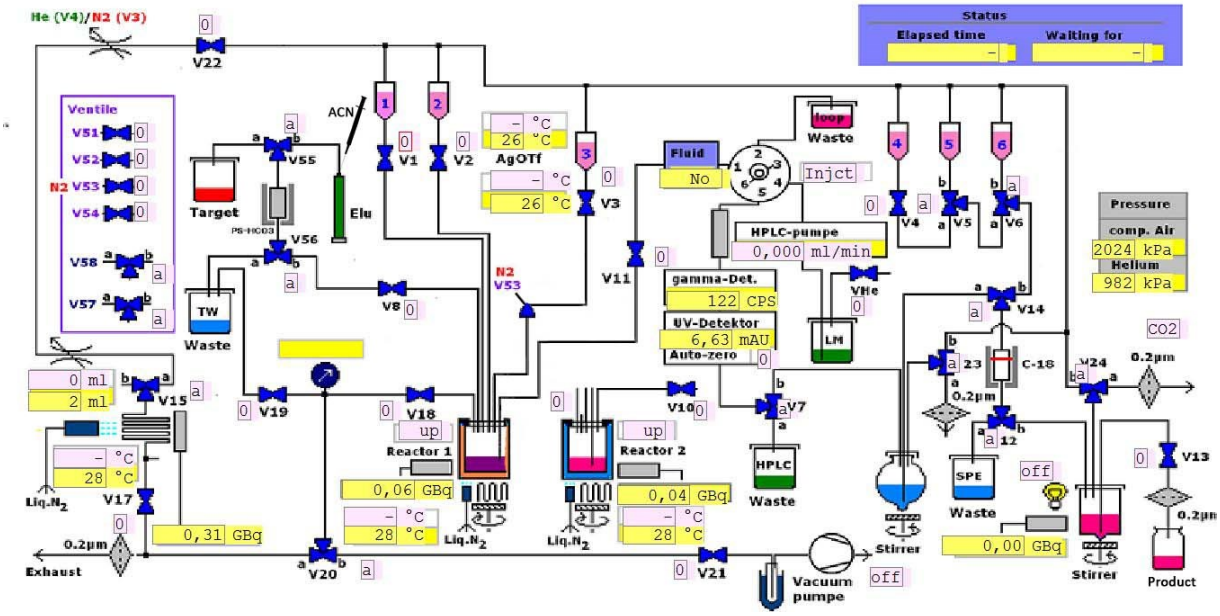

Figure 30: Scheme of the automated module.

Table 14: Description of symbols of the synthesis module.

Symbol	Name	Description
	Vials	Reagents are filled in the vials 1 - 6
	Valves	Transportation of gases and liquids (2 and 3 ways)
	Wheaton vial for elution	Vial for the elution and also acetonitrile for the azeotropic drying
	Wheaton vial with radioactivity	Vial filled with target activity in $H_2{}^{18}O$
	Bulb	Bulb filled with buffer mix for the collected peak
	Reactor	The reaction takes place here including heating, cooling and stirring
	Seperation cartridges	Preconditioned and conditioned cartriges for the solid phase extraction
	Product collecting vial	
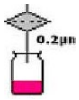	Product vial	Sterile filter adjusted

3.2.1.3.2 CLEANING OF THE MODULE

First the target vial was filled with deionized water and the “Elu”-vial with acetonitrile. With the help of the vacuum pump the Target was emptied via V55 and V56 to the TW Waste and then the Elu through V55, V56 and V8 into the reactor 1. The vacuum pump got turned off and with the help of the helium flow via V22, V1 and V11 the reactor 1 was emptied into the Loop waste. V1, V2 and V3 were cleaned two times with deionized water, two times with acetone and one time with acetonitrile. Therefore, the helium flow V22 needs to be open and then the liquids got pushed into the reactor 1 and again emptied through V11. The next step was the cleaning of the bulb with deionized water. Afterwards V4 and V6 were filled with water and V5 with ethanol. The liquid of V6 was pushed into the SPE waste and then V5 and V4 got washed into the product collecting vial. With the help of the helium flow V24 the solution got pushed through the final product line. Then all the lines were opened and the whole system dried with the helium flow V22 for a few minutes.

3.2.1.3.3 PRODUCTION OF [^{18}F]FLUORIDE ION

[^{18}F]F^- was obtained with the GE PETtrace™ cyclotron from GE Medical Systems. Therefore the nuclear reaction $^{18}O(p,n)^{18}F$ was used with [^{18}O]water as a target. The amounts of produced radioactivity varied from 10 to 55 GBq.

3.2.1.3.4 SYNTHESIS METHOD

Before the synthesis starts, all vials were filled with the chemicals shown in Table 15. Also, the Sep-Pak® cartridge was conditioned with ethanol (10 mL) followed by water (20 mL, B.Braun, Ecotainer®) and put into place between valve 14 and 12. The preconditioned separation cartridge PS-HCO_3 was assembled between valve 55 and 56. All wastes were emptied and a new glass vial and product vial were placed as shown in Figure 30. Liquid nitrogen was filled in the prescribed metal container.

Table 15: Amounts of chemicals for the preparation of the module.

Name of vial	Amount	Content
Elu vial	0.5 mL	Solution A*
Syringe placed in Elu vial	1.5 mL	Acetonitrile
V1	1 mL	Precursor in acetonitrile (4 mg/mL)
V2	0.3 mL	2 M KOH
V3	0.63 mL	Solution B**
V4	7.2 mL	NaCl 0.9%
V5	0.8 mL	EtOH
V6	20 mL	Solution C***
Bulb	60 mL	Solution C***

***Solution A:** 20 mg Kryprofix® 222 and 4.5 mg K_2CO_3 in 1 mL 80/20 acetonitrile/TraceSELECT® water (v/v)

****Solution B:** 30 µL AcOH in 600 µL of the preparative HPLC mobile phase

*****Solution C:** 60 mL phosphate buffer (0.1 M, pH = 7) + 120 µL ascorbic acid (500 mg L-ascorbic acid in 5 mL B.Braun water (Ecotainer®))

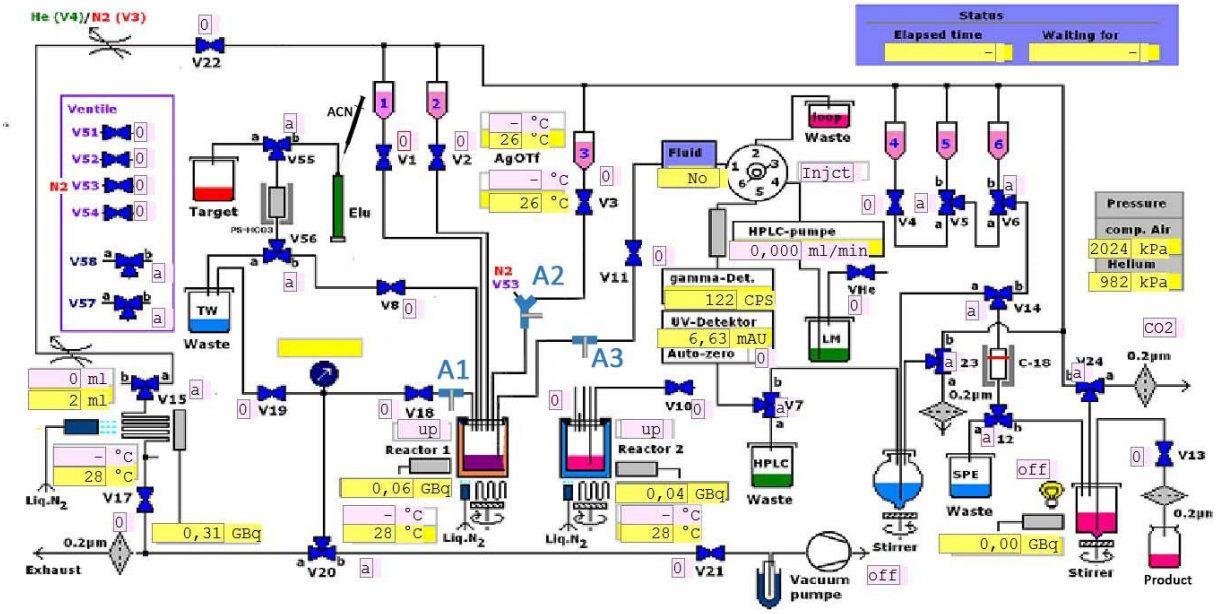

Figure 31: Scheme of the module including valves A1, A2 and A3.

The module has 3 valves, that needed to be opened and closed manually (Figure 31): There is one for the exhaust between V18 and the reactor (A1), one three-way valve connecting V53, V3 and the reactor (A2) and the last one was between the reactor and V11 (A3). Before the start of the synthesis, A3 was closed and A1/A2 were opened. After the preparation, the activity got connected to the module. The first step of the synthesis was the extraction of the [^{18}F]fluoride ion from the target water with the help of the separation cartridge PS-HCO_3. The target water was transferred into the TW waste. Then the first batch of acetonitrile (500 µL) from the syringe got pushed into the reactor 1 manually and the azeotropic drying started by heating up the reactor 1 to 120 °C. 3 azeotropic dryings were performed (500 µL CH_3CN each). Afterwards V1 was emptied with a constant helium flow of 50 ml/min into the reactor and A1 and A3 were closed manually. The mixture was stirred for 10 min at 100 °C and then for 5 min at 85 °C. Afterwards V2 was pushed into the reactor and solution was stirred at 90 °C for 5 min. When the reactor reached a temperature below the boiling point of acetonitrile, A1/A2/A3 were opened. V3 was transferred into the reactor and the entire reaction mixture was pushed through V11 into the HPLC loop. The fluid detector gave the signal to manually inject the liquid to the HPLC column. The next step was the collection of the product peak with the help of the radio detector by pressing STRG+S to start collecting the product by transferring it into the bulb. STR+T was pressed to stop collecting and to start purification and formulation. First the liquid of the bulb was pushed over the C-18 cartridge into the SPE Waste. V6, V5 and V4 were also pushed over the cartridge, whereas V6 was directed into the SPE Waste and V5/V4 were led to the product collecting vial. The last step of the synthesis was the transfer of the mixture into the final product vial (assembled with a sterile filter). Subsequently, the quality control

was performed. Decay-corrected (to the end of bombardment) radiochemical yield: 10 ± 3%. R_t = 4m27s (90:10:0.4 MeOH/H_2O/AcOH); R_f = 0.26 - 0.46 (100:10:0.4 MeOH/H_2O/CH_3COOH).

3.2.1.3.5 QUALITY CONTROL

The quality of the product was checked by HPLC, TLC, GC, Kryptofix test, pH and osmolality. The half-life was already measured after the production of fluorine-18. The required quality control tests with the acceptance criteria are shown in Table 16.

Table 16: Specifications and quality control of [^{18}F]FTHA.

Test	Acceptance criteria	Test method
Radiochemical purity		
Product [^{18}F]FTHA	≥ 95%	radio-HPLC
Free [^{18}F]fluoride ion	≤ 3%	
Product [^{18}F]FTHA	≥ 95%	radio-TLC
Free [^{18}F]fluoride ion	≤ 3%	
Chemical purity		
[^{19}F]FTHA	no values defined	UV-HPLC
Kryptofix 222	≤ 50 µg/mL	Kryptofix test
Radiochemical identity		
[^{18}F]FTHA	R_t = 4.5 ± 0.5 min	radio-HPLC
[^{18}F]FTHA	R_f = 0.4 ± 0.2	radio-TLC
Residual solvents		
Acetonitrile	< 410 ppm	GC
Methanol	< 3000 ppm	
Physical parameters		
pH	4.0 - 8.5	pH indicator strip
Osmolality	200 - 400 mosmol/kg	osmometer
Radionuclidic purity		
half-life	109.8 ± 10 min	dose calibrator
γ-spectrum	511 keV, 1022 keV	gamma spectrometer
Microbiological analysis		
Sterility	sterile	External lab (LAL-test, etc.)
Bacterial endotoxins	< 1.0 EU/mL	

Mobile phase: HPLC: 90:10:0.4 MeOH/H2O/AcOH; TLC: 100:10:0.4 MeOH/H2O/CH3COOH

3.2.1.3.6 STABILITY TESTS

The stability of the product was evaluated right after the synthesis, after 1 hour, 2 hours, 3 hours and 4 hours at room temperature by radio-HPLC and radio-TLC.

3.2.1.3.6.1 PLASMA STABILITY TEST

The plasma stability test was performed with frozen mouse plasma and frozen human serum. Everything was already frozen in batches for research by the Medical University of Vienna.

For the stability test the plasma and serum were always kept on ice. Three mixtures were prepared: the reference (tracer without plasma), the tracer with human serum and the tracer with mouse plasma. Four 1.5 mL Eppendorfer tubes were prepared: one with mouse plasma (290 µL), one with human serum (290 µL), one with pure [^{18}F]FTHA and the reference tube with saline solution (290 µL). They were incubated at 37 °C for at least 10 min. All mixtures were handled as followed. [^{18}F]FTHA (30 µL) was added to the prepared tube and shortly vortexed. Timepoint 0 was taken: 30 µL of the mix were placed in a tube containing acetonitrile (30 µL) and centrifuged for 5 min with 15000 rpm. It was evaluated by radio-HPLC. Another 3 timepoints were carried out after 1 hour, 2 hours and 3 hours. The procedure was identical to the one performed at timepoint 0.

3.2.1.3.7 SYNTHESIS PROTOCOL

For the automated module synthesis, a protocol and an instruction for the entire synthesis was prepared to track all necessary steps shown in chapter 6 (protocol in german).

3.2.2 [^{68}GA]GA-DATA^{5M}.SA.FAPI

3.2.2.1 PREPARATION OF THE PRECURSOR AND THE CHEMICALS

The precursor was dissolved in TraceSelect® water (1 mg/mL). The amount for the synthesis was prefilled in Eppendorfer tubes and kept in a common freezer. The 1 M ammonium acetate buffer (pH 5.5) was also prepared with TraceSelect® water and stored in the fridge.

3.2.2.2 SYNTHESIS OF [^{68}GA]GA-DATA^{5M}.SA.FAPI

Gallium-68, which was produced by the generator, was eluted into an evacuated 11 mL vial. Meanwhile, NH_4OAc buffer (150 µL, 1 M, pH 5.5) was added to the precursor in TraceSelect® water (15 – 42 µL, 20 – 42 nmol). The elution was added to the mixture and put on the thermo shaker at 30 °C for 15 min (700 rpm). [^{68}Ga]Ga-DATA^{5m}.SA.FAPi was diluted with PET phosphate buffer (125 mM) in the ratio 1:0.7 product/buffer. Subsequently, quality control was done. R_f = 0: ^{68}Ga-colloid, R_f = 1: [^{68}Ga]Ga-DATA^{5m}.SA.FAPi (1:1 1 M Ammonium acetate / methanol (pH 7.4)); R_t = 0.9 - 1.1 min: free gallium-68, R_t = 3.5 - 3.6 min: [^{68}Ga]Ga-DATA^{5m}.SA.FAPi (0.5 – 10 min, 5 – 95% CH_3CN (+0.1% TFA) / 95 – 5% H_2O (+ 0.1% TFA); 2 mL/min flow).

3.2.2.3 QUALITY CONTROL

The quality of the product was checked by radio-HPLC, radio-iTLC, pH and osmolality. The required quality control tests with the acceptance criteria are shown in Table 17.

Table 17: Specifications and quality control of [^{68}Ga]Ga-DATA^{5m}.SA.FAPi.

Test	Acceptance criteria	Test method
Radiochemical purity		
Product [^{68}Ga]Ga-DATA5m.SA.FAPi	≥ 93%	radio-HPLC
^{68}Ga-colloid	≤ 3%	
Product [^{68}Ga]Ga-DATA5m.SA.FAPi	≥ 93%	radio-TLC
Free gallium-68	≤ 4%	
Radiochemical identity		
[^{68}Ga]Ga-DATA5m.SA.FAPi	R_t = 3.6 ± 0.5 min	radio-HPLC
[^{68}Ga]Ga-DATA5m.SA.FAPi	R_f = 0.9 ± 0.1	radio-TLC
Physical parameters		
pH	4.5 – 7.0	pH indicator strip
Osmolality	200 – 400 mosmol/kg	osmometer
Radionuclidic purity		
half-life	1.13 ± 0.08 h	dose calibrator
γ-spectrum	511 keV, 1022 keV	gamma spectrometer
^{68}Ge-breakthrough	≤ 0.06%	gamma counter
Microbiological analysis		
Sterility	sterile	External lab (LAL-test, etc.)
Bacterial endotoxins	< 1.0 EU/mL	

Mobile phase: HPLC: 0.5 - 10 min, 5 - 95% CH_3CN (+0.1% TFA) / 95 - 5% H2O (+ 0.1% TFA); 2 mL/min flow;
TLC: 1:1 Ammonium acetate / methanol (pH 7.4)

3.2.2.4 STABILITY TESTS

The stability of the product was evaluated right after the synthesis, after 1 hour, 2 hours, 3 hours and 4 hours with radio-HPLC and radio-iTLC.

3.2.2.5 SYNTHESIS PROTOCOL

For the synthesis of [^{68}Ga]Ga-DATA^{5m}.SA.FAPi a protocol and an instruction for the entire synthesis was prepared to track all necessary steps shown in chapter 6 (protocol in german).

4 CONCLUSION AND OUTLOOK

The use of radiopharmaceuticals in medicine increases continuously and the need of research on novel ones is needed. PET imaging is a method for targeted imaging of desired processes in the body or to locate disease. The possibility to combine the imaging with therapeutics makes radiolabeling of compounds even more promising.

The radiolabeling to obtain both products, [^{18}F]FTHA and [^{68}Ga]Ga-DATA^{5m}.SA.FAPi, was conducted. To obtain [^{18}F]FTHA, fluorine-18 was produced by a cyclotron, radiolabeled *via* nucleophilic fluorination and characterized with radio-HPLC and radio-TLC. The synthesis including formulation of the product was conducted on an automated synthesis module (designed for ^{11}C syntheses) for *in vivo* studies with decay-corrected (to the end of bombardment) radiochemical yields of 10 ± 3%. To increase yields, the synthesis should be performed on an automated synthesis module that is designed for ^{18}F-fluorination. Furthermore, the stability of the radiotracer was investigated at room temperature and incubated with human serum and mouse plasma respectively. The characterization of the incubated tracer with mouse plasma showed an unknown side product, which need further investigation. To obtain [^{68}Ga]Ga-DATA^{5m}.SA.FAPi the chelator DATA^{5m} was complexed with gallium-68, which was produced *via* a generator. Characterization was done *via* radio-HPLC and radio-iTLC. The stability was determined over a period of 4 h and resulted in a fast decrease of product, but plasma stability tests to predict behavior in mammals still need to be investigated. Further research is necessary for improved *in vivo* studies and purification should be conducted before application. The selectivity to gallium-68 of the precursor could also be tested to avoid binding to iron when used in mammals. To avoid decomposition, the pH values of the whole synthesis and during stability tests could be tracked to minimize the formation of insoluble side products. An advantage of the radiolabeling with gallium-68 is the fast and easy handling.

Nevertheless, additional research is necessary to predict the behavior of both radiotracers in human. Both have a high potential in becoming routinely used radiopharmaceuticals for PET imaging of biological processes and disease respectively.

5 REFERENCES

(1) Bonka, H.; Narrog, J. Radioaktivität. Thieme Gruppe December 19, 2012.
(2) Wiberg, N. *Lehrbuch Der Anorganischen Chemie*, 102nd ed.; Walter de Gruyter & Co.: Berlin, 2007.
(3) Lieser, K. H. *Nuclear and Radiochemistry*, 2nd ed.; WILEY-VCH, 2001.
(4) Mortimer, C. E.; Müller, U. *Chemie*, 11th ed.; Thieme: Stuttgart, 2014.
(5) Kónya, J.; Nagy, N. M. *Nuclear and Radiochemistry*; Elsevier, 2012.
(6) Saha, G. B. *Fundamentals of Nuclear Pharmacy*, 6th ed.; Springer: Cleveland, OH 44195, USA, 2010.
(7) Jacobson, O.; Kiesewetter, D. O.; Chen, X. Fluorine-18 Radiochemistry, Labeling Strategies and Synthetic Routes. *Bioconjugate Chemistry* **2015**, *26* (1), 1–18. https://doi.org/10.1021/bc500475e.
(8) Meisenheimer, Michael; Saenko, Yury; Eppard, E. Gallium-68: Radiolabeling of Radiopharmaceuticals for PET Imaging - A Lot to Consider. In *Medical Isotopes*; IntechOpen, 2019; pp 1–21. https://doi.org/10.5772/intechopen.90615.
(9) Roesch, F.; J. Riss, P. The Renaissance of the 68Ge/68Ga Radionuclide Generator Initiates New Developments in 68Ga Radiopharmaceutical Chemistry. *Current Topics in Medicinal Chemistry* **2012**, *10* (16), 1633–1668. https://doi.org/10.2174/156802610793176738.
(10) Morgat, C.; Hindié, E.; Mishra, A. K.; Allard, M.; Fernandez, P. Gallium-68: Chemistry and Radiolabeled Peptides Exploring Different Oncogenic Pathways. *Cancer Biotherapy and Radiopharmaceuticals* **2013**, *28* (2), 85–97. https://doi.org/10.1089/cbr.2012.1244.
(11) Tsionou, M. I.; Knapp, C. E.; Foley, C. A.; Munteanu, C. R.; Cakebread, A.; Imberti, C.; Eykyn, T. R.; Young, J. D.; Paterson, B. M.; Blower, P. J.; Ma, M. T. Comparison of Macrocyclic and Acyclic Chelators for Gallium-68 Radiolabelling. *RSC Advances* **2017**, *7* (78), 49586–49599. https://doi.org/10.1039/c7ra09076e.
(12) Welch, M. J.; Redvanly, C. S. *Handbook of Radiopharmaceuticals*; Wiley: West Sussex, England, 2003.
(13) Blower, P. J.; Cusnir, R.; Darwesh, A.; Long, N. J.; Ma, M. T.; Osborne, B. E.; Price, T. W.; Pellico, J.; Reid, G.; Southworth, R.; Stasiuk, G. J.; Terry, S. Y. A.; de Rosales, R. T. M. Gallium: New Developments and Applications in Radiopharmaceutics. In *Advances in Inorganic Chemistry*; Academic Press, 2021; pp 1–35. https://doi.org/10.1016/bs.adioch.2021.04.002.
(14) Lu, F.-M.; Yuan, Z. PET/SPECT Molecular Imaging in Clinical Neuroscience: Recent Advances in the Investigation of CNS Diseases. *Quant Imaging Med Surg* **2015**, *5* (3), 433–447. https://doi.org/10.3978/j.issn.2223-4292.2015.03.16.
(15) Gemmell, H. G.; Staff, R. T. Single Photon Emission Computed Tomography (SPECT). In *Practical Nuclear Medicine*; Springer: London, 2005; pp 21–34.
(16) Choppin, G.; Liljenzin, J.-O.; Rydberg, J.; Ekberg, C. Uses of Radioactive Tracers. In *Radiochemistry and Nuclear Chemistry*; Elsevier, 2013; pp 545–593.
(17) Sharp, P. F.; Welch, A. Positron Emission Tomography (PET). In *Practical Nuclear Medicine*; Springer: London, 2005; pp 35–48.
(18) Cherry, S. R. Multimodality Imaging: Beyond PET/CT and SPECT/CT. *Semin Nucl Med* **2009**, *39* (5), 348–353. https://doi.org/10.1053/j.semnuclmed.2009.03.001.
(19) Vermeulen, K.; Vandamme, M.; Bormans, G.; Cleeren, F. Design and Challenges of Radiopharmaceuticals. *Seminars in Nuclear Medicine* **2019**, *49* (5), 339–356. https://doi.org/10.1053/j.semnuclmed.2019.07.001.
(20) Lopaschuk, G.; Ussher, J.; Folmes, C.; Jaswal, J.; Stanley, W. Myocardial Fatty Acid Metabolism in Health and Disease. *Physiological reviews* **2010**, *90*, 207–258. https://doi.org/10.1152/physrev.00015.2009.
(21) Savisto, N.; Viljanen, T.; Kokkomäki, E.; Bergman, J.; Solin, O. Automated Production of [18F]FTHA According to GMP. *Journal of Labelled Compounds and Radiopharmaceuticals* **2018**, *61* (2), 84–93. https://doi.org/10.1002/jlcr.3589.
(22) van der Vusse, G. J. Albumin as Fatty Acid Transporter. *Drug Metabolism and Pharmacokinetics* **2009**, *24* (4), 300–307. https://doi.org/10.2133/dmpk.24.300.
(23) Takala, T. O.; Nuutila, P.; Pulkki, K.; Oikonen, V.; Grönroos, T.; Savunen, T.; Vähäsilta, T.; Luotolahti, M.; Kallajoki, M.; Bergman, J.; Forsback, S.; Knuuti, J. 14(R,S)-[18F]Fluoro-6-Thia-Heptadecanoic Acid as a Tracer of Free Fatty Acid Uptake and Oxidation in Myocardium and Skeletal Muscle. *European Journal of Nuclear Medicine* **2002**, *29* (12), 1617–1622. https://doi.org/10.1007/s00259-002-0979-y.
(24) Pandey, M. K.; Jacobson, M. S.; Groth, E. K.; Tran, N. G.; Lowe, V. J.; DeGrado, T. R. Radiation Induced Oxidation of [18F]Fluorothia Fatty Acids under CGMP Manufacturing Conditions. *Nuclear Medicine and Biology* **2020**, *80–81*, 13–23. https://doi.org/10.1016/j.nucmedbio.2019.11.004.
(25) Fitzgerald, A. A.; Weiner, L. M. The Role of Fibroblast Activation Protein in Health and Malignancy. *Cancer Metastasis Rev* **2020**, *39* (3), 783–803. https://doi.org/10.1007/s10555-020-09909-3.

(26) Hamson, E. J.; Keane, F. M.; Tholen, S.; Schilling, O.; Gorrell, M. D. Understanding Fibroblast Activation Protein (FAP): Substrates, Activities, Expression and Targeting for Cancer Therapy. *Proteomics - Clinical Applications* **2014**, *8* (5–6), 454–463. https://doi.org/10.1002/prca.201300095.
(27) Lindner, T.; Loktev, A.; Giesel, F.; Kratochwil, C.; Altmann, A.; Haberkorn, U. Targeting of Activated Fibroblasts for Imaging and Therapy. *EJNMMI Radiopharmacy and Chemistry* **2019**, *4* (1), 1–15. https://doi.org/10.1186/s41181-019-0069-0.
(28) Moon, E. S. Targeting Fibroblast Activation Protein (FAP): Next Generation PET Radiotracers Using Squaramide Coupled Bifunctional DOTA and DATA5m Chelators. **2020**, *5* (19), 1–35. https://doi.org/10.21203/rs.3.rs-24915/v1.
(29) Moon, E. S.; Van Rymenant, Y.; Battan, S.; De Loose, J.; Bracke, A.; Van der Veken, P.; De Meester, I.; Rösch, F. In Vitro Evaluation of the Squaramide-Conjugated Fibroblast Activation Protein Inhibitor-Based Agents AAZTA5.SA.FAPi and DOTA.SA.FAPi. *Molecules* **2021**, *26* (12), 3482. https://doi.org/10.3390/molecules26123482.
(30) Byram, M.; Holmes, P.; Savvides, N. Equilibrium, Kinetic and Structural Properties of Gallium(III)- and Some Divalent Metal Complexes Formed with the New DATAm and DATA5m Ligands. *Language learning journal* **2013**, *41* (3), 251–253.
(31) Brom, M.; Franssen, G. M.; Joosten, L.; Gotthardt, M.; Boerman, O. C. The Effect of Purification of Ga-68-Labeled Exendin on in Vivo Distribution. *EJNMMI Research* **2016**, *6* (1), 1–8. https://doi.org/10.1186/s13550-016-0221-8.
(32) Velikyan, I.; Sundin, A.; Sörensen, J.; Lubberink, M.; Sandström, M.; Garske-Román, U.; Lundqvist, H.; Granberg, D.; Eriksson, B. Quantitative and Qualitative Intrapatient Comparison of 68Ga-DOTATOC and 68Ga-DOTATATE: Net Uptake Rate for Accurate Quantification. *J Nucl Med* **2014**, *55* (2), 204–210. https://doi.org/10.2967/jnumed.113.126177.
(33) Fowler, J. S. 18F-FDG Radiosynthesis: A Landmark in the History of PET. *J Nucl Med* **2020**, *61* (Supplement 2), 105–109. https://doi.org/10.2967/jnumed.120.250191.
(34) Goud, N. S.; Joshi, R. K.; Bharath, R. D.; Kumar, P. Fluorine-18: A Radionuclide with Diverse Range of Radiochemistry and Synthesis Strategies for Target Based PET Diagnosis. *European Journal of Medicinal Chemistry* **2020**, *187*, 1–45. https://doi.org/10.1016/j.ejmech.2019.111979.
(35) Yu, S. Review of 18F-FDG Synthesis and Quality Control. *Biomed Imaging Interv J* **2006**, *2* (4), 57. https://doi.org/10.2349/biij.2.4.e57.
(36) Di, L.; Kerns, E. H.; Hong, Y.; Chen, H. Development and Application of High Throughput Plasma Stability Assay for Drug Discovery. *International Journal of Pharmaceutics* **2005**, *297* (1–2), 110–119. https://doi.org/10.1016/j.ijpharm.2005.03.022.

6 ATTACHMENTS

6.1 SYNTHESIS PROTOCOL OF [^{18}F]FTHA

MEDIZINISCHE UNIVERSITÄT WIEN — Allgemeines Krankenhaus der Stadt Wien

UNIVERSITÄTSKLINIK FÜR RADIOLOGIE UND NUKLEARMEDIZIN
Klinische Abteilung für Nuklearmedizin

[^{18}F]FTHA_ HerstProtokoll **RADNUK-NUK-FM**
gültig ab: 09.09.2020 Version: 01 Seite **1** von **4**

[^{18}F]FTHA-Charge: _____ **Datum** : _____

Herstellung

Zyklotron run: _____ Targetaktivität: _____GBq@___:___Uhr Synthesestart:_____

FTHA-Ausbeute: ____GBq (__:__Uhr) ___% (unkorr.) Aktivitätskonz.: _____ MBq /mL

PET-Labor

Zelle A: Verpressung AN	O
GLS: Zelle A - Auslass - F minus	O
nach Delivery: FDG - Auslass	O
Synthesedaten eintragen in Liste (Bestrahlung außerhalb der Routine)	O

Labor

He, DR und N_2 an (He-Pressure ~ 60 kPa)	O
Präparative HPLC: richtige Laufmittel- und Säulenposition konditioniert; wenn nicht dann zuerst Spülen auf Waschposition (850:150:4:2=MeOH:H_2O:Acetic acid:Ascorbic acid)	O
Nuclear Interface Modul gereinigt, Syntheseprogramm FTHA gestartet, Vorbereitung komplett	O
C18 light Kartusche mit 10 mL Ethanol und 20 mL Wasser konditioniert	O
Analyt. HPLC eingestellt und konditioniert : Laufmittel (90 :10 :0.4 = MeOH :H_2O :CH_3COOH), Gemini® 10µm C18 110Å Säule, flow 1,8 mL/min) ; UV-Detekor auf 230 nm	O
DC vorbereitet (TLC Silicagel 60 RP-18, Laufmittel: 100:5:0,4=MeOH:H_2O:CH_3COOH)	O
Eppi, Spritze vorbereitet für Qualitätskontrolle	O
Flüssiger N_2 nachgefüllt	O
Synthesedaten F-18 Produktionen eingetragen	O
Kontaminationsmessung durchgeführt	O
Nach Synthese: V2 mit Wasser über V11 waschen	O
Ausreichende Gasdrücke (He, Ar und N_2) nach der Synthese	O

DVR: 0000191

Synthese

Verwendete Materialien	Menge	Charge laut Liste
F-18 Kartusche	1	O
C18 light SepPak an Steckplatz	1	O
Elutionslösung: 20 mg Kryptofix; 4,5 mg K_2CO_3 pro 1 mL 80/20 Acetonitril/Wasser (v/v) in Wheoton Vial	0.5 mL	O
Acetonitril (f. azeotr. Trocknung) in Spritze in Eluvial	1.5 mL	O
V1: Precursor in Acetonitril (4 mg/mL)	1 mL	O
V2: 2M KOH	0.3 mL	O
V3: CH_3COOH (30 µL) in Laufmittel (präp. HPLC) (600 µL)	0.63 mL	O
Bulb: Phosphatpuffer-Ascorbinsäure Mix	60 mL	O
V4: NaCl 0,9%	7.2 mL	O
V5: Ethanol	0.8 mL	O
V6: Phosphatpuffer-Ascorbinsäure Mix	20 mL	O
Produktvial beschriftet mit Sterilfilter (gelb) assembliert	1	O

Phosphatpuffer: 0.1 M; pH=7
Ascorbinsäure: 500 mg pro 5 mL
Phosphatpuffer-Ascorbinsäure Mix: 60 mL Puffer + 120 µL Ascorbinsäure

Bemerkungen:

Akt. [^{18}F] KF/K_{222} (vor AZT Re1):……GBq (……Uhr)

Akt. [^{18}F] KF/K_{222} (nach AZT Re1):……GBq (……Uhr)

Akt. [^{18}F]FTHA (nach KOH):……GBq (……Uhr)

Durchführende Person Herstellleiter

Modul	
Magnetrührer in Reaktor 1	O
Reaktor in Heizblock	O
Exhaust 1 + Y offen; Line über Reaktor 1 geschlossen	O
Waste entleert bzw. $H_2{}^{18}O$ in den Sammelbehälter	O
Loop waste vial und Produktvial an Position	O
Nadel im Targetgefäß	O

[^{18}F]FTHA-Charge: _____ **Datum** : _____

Qualitätskontrolle

	Entspricht	Entspricht nicht	Wert
RCR (HPLC - Radioaktivitätsdetektor)			
Produkt [^{18}F]FTHA ≥95%	☺	☐	_____ % R_t=_____
Freies [^{18}F]Fluorid ≤3%	☺	☐	_____ % R_t=_____
Sonstige Verunreinigungen	☺	☐	_____ % R_t=_____
RCR (DC – MeOH/H_2O/CH3COOH = 100:5:0,4)			
Produkt [^{18}F]FTHA ≥95%	☺	☐	_____ % R_f=_____
[^{18}F]Fluorid ≤3%	☺	☐	_____ % R_f=_____
Chemische Reinheit (HPLC – UV Det)			
[^{19}F]FTHA	☺	☐	_____ µg/mL
Precursor			_____ µg/mL
Kryptofix ≤50µg/mL	☺	☐	_____ µg/mL
Prüfung auf Lösungsmittel (GC - FID)			
Acetonitril < 410 ppm	☺	☐	_____ppm t_R=…….min
Methanol < 3000 ppm	☺	☐	_____ppm t_R=…….min
Ethanol	☺	☐	t_R=…….min
„Aqueous“ Peak	☺	☐	t_R=…….min
Physikalische Parameter			
pH-Wert 4.0 - 8.5	☺	☐	_____
Osmolalität 200-400 mosm/kg	☺	☐	_____mosmol/kg
Radionuklidische Reinheit	☺		
HWZ ($t_{½}$) 109.8 ± 10 min		☐	_____min
γ-Spektrum Linien: 511 & 1022 keV	☺	☐	_____keV
FREIGABE DER CHARGE	**JA** ☺	**NEIN** ☐	

Anmerkungen zur QK:

Mikrobiologische Untersuchungen Sterilität gewährleistet	☺	☐	
Endotoxine <1.0 EU/mL	☺	☐	

Qualitätskontrolleur: Kontrollleiter:

6.2 INSTRUCTION FOR THE AUTOMATED MODULE SYNTHESIS OF [^{18}F]FTHA

1 GELTUNGSBEREICH UND ZWECK

Dieses Dokument gilt für den Radiochemie- und Radiopharmazie-Bereich der Universitätsklinik für Radiologie und Nuklearmedizin, Klinische Abteilung für Nuklearmedizin (3L und 2V) der Medizinischen Universität Wien und des Allgemeinen Krankenhauses der Stadt Wien.

Ziel ist der korrekte Ablauf der gegenständlichen Tätigkeit (Synthese, Qualitätskontrolle, etc.)

2 MITGELTENDE DOKUMENTE

[^{18}F]FTHA_HerstProtokoll_FM

3 VORBEREITUNG/VERBRAUCHSMATERIAL

Siehe Punkt 6

4 VERWENDETE ABKÜRZUNGEN/ BEGRIFFE VERANTWORTLICHKEIT

MA	Mitarbeiter
QB	Qualitätsbeauftragter
AL	Abteilungsleiter
HL	Herstelleiter
ca.	cirka
mind.	Mindestens
mM	Millimol pro Liter
GLS	Gasleitsystem
µA	Mikroampere
mL	Milliliter
H_2O	Wasser (Aqua Bidest)
SCX	Strong Cation exchange
µL	Mikroliter
N_2	Stickstoff
µm	Mikrometer
mm	Millimeter
GC	Gaschromatograph
GBq	Gigabequerel
HPLC	Hochdruckflüssigkeitschromatographie

5 VERANTWORTLICHKEIT

- Für den Herstellungsprozess des Radiopharmakons, [^{18}F]FTHA trägt der Herstelleiter die Verantwortung; für die ordnungsgemäße Durchführung der Qualitätskontrolle und Freigabe der Charge der Kontrolleiter des PET-Zentrums.

Der Herstelleiter muss die geeignete Einschulung von jedem [^{18}F]FTHA-Hersteller garantieren. Dazu muss jeder [^{18}F]FTHA-Hersteller einen Schulungsnachweis für alle dabei verwendeten Geräte (Synthese und Qualitätskontrolle) vorweisen können: Zyklotron, Nuclear Interface Modul, HPLC, Osmometer, pH-meter, γ-Spektrometer, Gaschromatograph und DC-miniGITA Scanner.

6 ARBEITSABLAUF/TÄTIGKEITSBESCHREIBUNG

Vorbereitung Zyklotron und Bestrahlungsstart, ^{18}F-Gewinnung:

⇒ Gasleitsystem und Masterkonsole aktivieren

⇒ Verpressung Zelle A einschalten.

⇒ *Auslass Zelle A (rot) am GLS anwählen, F minus*

⇒ Wheaton Vial (min 2,5 mL) mit Entlüftungskanüle an die Targetentleerungsleitung (=Spülleitung, =F18-Waste) anschließen.

⇒ Bleigefäß für späteren Transport in der Zelle vorbereiten.

⇒ *Maintainance → PETTrace → Start Up H (takes a few minutes)*
Production → 18F self shielded (takes a few minutes)

⇒ *Start irradiation*

⇒ Wenn genug bestrahlt (Anzeige am Computer), dann *Delivery (check F minus to cell A)*
Delivery in die Zelle A mit gleichzeitigem Kontrollblick ob die ^{18}F-Aktivität über die Wasteleitung ins Auffanggefäß transportiert wird.

⇒ Messen der Aktivität im kalibrierten Dosiskalibrator (notieren als Startaktivität).

⇒ Warten bis Targetentleerung beendet ist und 10-15 Minuten warten

⇒ Transfer in Blei- bzw. Wolframgefäß und Ausschleusen aus der Zelle A für weiteren Transport zum Nuclear Interface Modul. In den Lift geben.

⇒ Gegebenenfalls Verpressung Zelle A, Zyklotron und Gasleitsystem ausschalten.

Vorbereitung Modul

⇒ Das Nuclear Interface Modul einschalten und die Gasversorgung (He, N_2, Ar und Druckluft) sicherstellen. Das Steuerungsprogramm starten. Vakuumpumpe oberhalb der Zelle einschalten.

⇒ Reinigung der Leitungen für die ^{18}F-Fixierung

Target Water (TW)-Waste Vial kontrollieren: falls noch von vorheriger Synthese voll: Inhalt in dafür vorgesehenen Sammelbehälter zwecks [^{18}O]H_2O Rückgewinnung entleeren und Vial erneut konnektieren. Falls das Septum undicht ist, wird dieses getauscht und mit 2 rosa Nadeln assembliert (an V56, TW-Waste anstecken).

Target Water (TW)- Vial- mit H_2O befüllen und mit Vakuum über V55→a und V56→a in das TW-Waste Vial spülen. Dazu Vakuumpumpe aufdrehen und über V21→1, V20→b und V19→1 ansaugen.

Anschließend Vakuum abdrehen und Ventile auf Ausgangsstellung setzen. Anschließend wird das Elu-Vial mit ACN befüllt und über V55→b V56→b, V8→1, V18→1, V20→b und V21→1 in den Reaktor (Re) 1 gewaschen. Ventile zurückstellen und Vakuum schließen. Reaktor 1 über V11→1 und V1→1 mit einem He Strom in den HPLC-Waste entleeren.

TW Waste Gefäß entleeren

⇒ Reinigung des Moduls

V1, V2, V3 mit Helium aus V22 in den Re 1 mit H_2O (2-mal), Aceton (2-mal) und ACN (1-mal) waschen, entleeren über die *Needle* Richtung V11 in das HPLC-Wastegefäß (jeweils *Inject* und *Load* Position waschen).

Bulb mit H_2O waschen und dann füllen; entleeren über V14 und V12 in das SPE-Wastegefäß.

V6 mit Hilfe des V22 Helium in den SPE Waste entleeren.

V5 mit Helium aus V22 in das Produktgefäß mit Ethanol waschen, entleeren über V13 in ein SPE-Wastegefäß.

V4 mit Helium aus V22 mit H_2O in das SPE-Wastegefäß waschen.

⇒ Vorbereitung der ^{18}F-Fixierung

Elu-(=Elutionslösung)-Vial mit gelber Nadel an V55→Elu Leitung anstecken. Mit 500 µL Elutionslösung befüllen (20 mg K.2.2.2 (Kryptofix 2.2.2.) und 4,5 mg K_2CO_3 (Kaliumcarbonat) werden in 800 µL ACN und 200 µL H_2O (TraceSelect, über PS-HCO_3 gefiltert) aufgelöst).

⇒ Neue PS-HCO_3^- (45 mg) Kartusche zwischen V55 und V56 (links oben) assemblieren.

⇒ Vorbereitung der Synthese

Ein 2,2 mL Vial für die Radioaktivität vorbereiten.

In der Schleuse wird ein Bleitopf zum Transport ins PET Zentrum vorbereitet.

Reagenzien einfüllen

Vorratsgefäß V1 (erst unmittelbar vor Synthese): 1 mL Precursor (4 mg/mL in ACN).

Vorratsgefäß V2: 300 µL 2M KOH.

Vorratsgefäß V3: 30 µL Essigsäure in 600 µL mobile Phase der präparativen HPLC.

Vorratsgefäße V4: 9 mL NaCl 0,9%.

Vorratsgefäße V5: 1 mL Ethanol.

Vorratsgefäße V6: 20 mL Phosphatpuffer-Ascorbinsäure Mix.

Bulb: 60 mL Phosphatpuffer-Ascorbinsäure Mix.

An den Kartuschen Steckplatz: C18 light SepPak .

An die V13 Leitung wird über eine rosa Kanüle ein 25 mL Produktvial mit rosa Ausgleichskanülen und Sterilluftfilter versehen.

⇒ Heat/Cool, UV Detektor und Vakuumpumpe werden durch die entsprechenden Schalter oberhalb der Zelle mit Strom versorgt, erst kurz vor Synthese einschalten.

⇒ Flüssigen Stickstoff nachfüllen und Dichtigkeit prüfen.

^{18}F-Fixierungsvorgang im Nuclear Interface

⇒ Kontrolle, ob die Kanülen in den entsprechenden Gefäßen richtig assembliert sind. Ventil zu V11 geschlossen.

⇒ Die transferierte Aktivität wird an TW-V55-Leitung angeschlossen und das Programm FTHA gestartet.

⇒ Ventil 55 wird in Richtung TW geschalten, V56 Richtung V19 und V20 in Richtung Vakuumpumpe, welche zuletzt mit V21 angeschlossen wird.

⇒ Ventile werden nach dem Transfer über die Anionenaustauschersäule in Ausgangsposition geschalten und die Vakuumpumpe abgeschaltet.

⇒ Für die Elution in den Reaktor wird der Leitungsweg in Richtung V55→b, V56→b, V8→1, manueller 3-Wegehahn offene Position, V18→1, V20→b und V21→1 geschalten, durch die Vakuumpumpe wird die Aktivität in den Reaktor 1 gesaugt.

⇒ Wenn Targetgefäß entleert und V8 noch offen, dann 0,5 mL ACN mittels der bereits assemblierten Spritze in das Elu-Vial hinzufügen.

⇒ Nach automatisierter azeotroper Trocknung wird auf 40 °C gekühlt. Während der azeotropen Trocknung kann die nächste Portion 0,5 mL ACN in das Elu-Vial gegeben werden. Dieser Schritt wird 2 Mal wiederholt, um die 3 azeotropen Trocknungen durchzuführen.

[^{18}F]FTHA Reaktion:

⇒ Über V1 wird mit Hilfe des V22 Heliums der Precursor in ACN (4 mg/mL) in den Re1 geleitet. Anschließend wird der Stickstoff 3-Wegehahn und der Exhaust geschlossen. Der Re1 wird auf 100 °C erhitzt und nach 10 min auf 85 °C gekühlt und für 5 min weitergerührt.

⇒ Exhaust wird kurz geöffnet (bei Temperatur 50) und über V2 wird 2M KOH in den Re1 geleitet. Wenn V2 leer ist, dann Exhaust schließen.

⇒ Re1 wird auf 90°C erhitzt und es wird für 4 Minuten gerührt. Wenn Temperatur um 50°C: Leitung zu V11, der Exhaust und der 3 Wegehahn werden anschließend geöffnet.

⇒ Über V3 wird Essigsäure verdünnt in dem Laufmittel der präp. HPLC hinzugefügt und kurz gerührt. V11 wird geöffnet und über Needle down die Reaktionsmischung auf die HPLC aufgetragen. (Fluid-Detektor beobachten und sobald keine Flüssigkeit mehr erkannt wird manuell *Inject* drücken)

⇒ HPLC Radiochannel muss beobachtet werden und der Peak bei ungefähr 7 Minuten gesammelt werden (STRG+S=Start collecting; STRG+T=stop collecting).

⇒ Der Bulb mit dem gesammelten Peak wird über V14->b und V12->a mit Hilfe des Vakuums (V23->b) über die C18 light Kartusche geleitet - immer beobachten und wenn nötig mit F2 die Synthese anhalten, um den gesamten Bulb zu leeren. Dann wird mit Phosphatpuffer aus V6 über V14 und V12 in den SPE Waste nachgewaschen.

⇒ Das Produkt wird mit EtOH aus V5 eluiert und mit 9 mL NaCl aus V4 nachgewaschen.

⇒ Die Produktlösung über V13 in das dafür vorbereitete 25 mL Vial transferiert und im Bleitopf ausgeschleust.

⇒ Anschließend wird das Produkt im Dosiskalibrator gemessen (Produktaktivität).

⇒ V2 wird nach Beendigung mit Wasser gewaschen.

⇒ Programm beenden und Laptop herunterfahren.

⇒ Gasversorgung, Heat/Cool, UV Detektor und Vakuumpumpe ausschalten.

Entnahme der Qualitätskontrollproben und Qualitätskontrolle

⇒ Mit einer 1 mL-Spritze und einer gelben Kanüle wird eine Probe in das Eppi (ca. 0,4 mL) transferiert.

⇒ Qualitätskontrolle durchführen (analytische HPLC, radioTLC, GC, pH, Osmolalität, γ-Spektrum, Kryptofix und HWZ Bestimmung).

⇒ (Radio)chemische Reinheitsbestimmung:

Radio-RI-HPLC-Methode: FTHA.

Säule: Gemini® 10µm C18 110Å Säule; Mobile Phase: 90 :10 :0.4 = MeOH :H2O :CH3COOH

Flußrate: (1,8 mL/min)

Rt ([^{18}F]F^-): 2,5-2,6 min

Rt ([^{18}F]FTHA): 4,4-4,6 min

Rt ([^{19}F]FTHA): 4,4-4,6 min (UV-channel)

Rt (Precursor): 7,0 min (UV-channel)

⇒ Radio-DC:

DC-miniGITA: FTHA

DC-Aluminium Platte: Kiesel Gel 60 RP-18

Flüssige Phase: 100:5:0,4=MeOH:H2O:CH3COOH

Rf ([^{18}F]F^-): 0-0.1

Rf ([^{18}F]FTHA): 0.1-0.5

⇒ pH-Bestimmung: mit pH Meter (4 – 8,5)

⇒ Osmolalität: mit Osmometer (200 – 400 mosm/kg)

⇒ Radionuklidische Reinheit: mit Gamma-Spektrometer (480-530 keV) und ausgerechnete Halbwertszeit: 3 Messungen innerhalb 15 Minuten (109.8±10 min).

⇒ Kryptofix Gehalt: mit Kryptofix Spot Test (≤50 µg/mL)

⇒ Acetonitril und Ethanol Gehalt

FID-GC Methode: FDG

Rt (Ethanol): 0.89-1 min

Rt(Methanol) : 0.8-0,9 min

Rt (Acetonitril): 1.06-1.26 min

⇒ Abweichungen von den Sollwerten sind dem Kontrolleiter unverzüglich mitzuteilen.

7 ERLÄUTERUNGEN

8 ÄNDERUNGEN

Datum	Version	Änderung
28.09.2020	01	Erstellung

6.3 SYNTHESIS PROTOCOL [^{68}GA]GA-DATA^{5M}.SA.FAPI

UNIVERSITÄTSKLINIK FÜR RADIOLOGIE UND NUKLEARMEDIZIN
Klinische Abteilung für Nuklearmedizin

MEDIZINISCHE UNIVERSITÄT WIEN

Allgemeines Krankenhaus der Stadt Wien

[^{68}Ga]GaFAPi_HerstProtokoll		RADNUK-NUK-FM
gültig ab: 24.09.2020	Version 01	Seite 1 von 3

[^{68}Ga]GaFAPi - Charge : _____ Datum.....

Herstellung:

Generator Elutionsnr : _____ Aktivität _____MBq _____:_____Uhr

Synthesestart:_____:_____Uhr Ausbeute:_____ MBq _____:_____Uhr _____% (unkorr.)

Thermoschüttler vorgeheizt auf 30°C	O
1M NH_4OAc Puffer (pH 5.5) vorbereitet	O
Precursor (20 µg) in 20 µL Aqua trace select gelöst (vorgefertigte 1 mg/ml Lösung)	O
150 µL Puffer zu Precursor-Lösung gegeben	O
Elution des Generators/der Generatoren erfolgt	O
Start der Synthese im Protokoll vermerkt	O
HPLC 1: Pumpe ein; UV-Detektor (220 nm) ein; LM A + B Kontrolle	O
DC: 1 iTLC-SG Streifen vorbereitet; Laufmitteltrog befüllt; Autoradiograph bereit	O

[^{68}Ga]GaFAPi - Charge:_____ Datum.....

Verwendete Reagentien / Verbrauchsmittel	Menge	Charge laut Liste
Precursor (20 µg) in 20 µL Aqua trace select	1	O
NH_4OAc (1M, pH 5.5)	150 µL	O
Generatoreluat	1 mL	O
Eppi für Reaktion beschriftet	1	O
PET-Phosphatpuffer 125 mM (1:0,7 Verdünnung)	819 µL	O
Reaktionsvial (ABX 11 mL), beschriftet	1	O
Eppi für die Qualitätskontrolle, beschriftet	1	O

Bemerkungen:

	Funktion	Name oT	Datum	Unterschrift
erstellt	Master	Hannah Kanatschnig	24.09.2020	e.h.
geprüft-inhaltlich				e.h.
geprüft-inhaltlich				e.h.
geprüft-formal				e.h.
geprüft-formal				e.h.
freigegeben-final				e.h.

6.4 INSTRUCTION FOR THE SYNTHESIS OF [^{68}GA]GA-DATA^{5M}.SA.FAPI

1 GELTUNGSBEREICH UND ZWECK

Dieses Dokument gilt für den Radiochemie- und Radiopharmazie-Bereich der Universitätsklinik für Radiologie und Nuklearmedizin, Klinische Abteilung für Nuklearmedizin (3L und 2V) der Medizinischen Universität Wien und des Universitätsklinikums Allgemeines Krankenhaus der Stadt Wien.

Ziel ist der korrekte Ablauf der gegenständlichen Tätigkeit (Synthese, Qualitätskontrolle, etc.)

2 MITGELTENDE DOKUMENTE

RADNUK – NUK – FM: [^{68}Ga]GaFAPi_HerstProtokoll"
RADNUK – NUK _ AA ,,Reinigung und Desinfektion im Radiochemiebereich"
RADNUK – NUK – AA: Arbeitsablauf LAF Radiopharmakologie
Messung mit dem Osmometer_AA
Laborordnung PET

3 VORBEREITUNG/VERBRAUCHSMATERIAL

Precursor
TraceSelect Wasser
Ammoniumacetat
PET Phosphatpuffer 125 mM
GalliAd oder EZAG Generatoren
1 steriles evakuiertes Gefäß; 11 mL (ABX)

DC Laufmittel:
1 M Ammoniumacetat, pH 5,5 + MeOH (1:1)

HPLC Laufmittel:
Lösung A (Aqua bidestillata + 0,1% TFA), Lösung B (ACN + 0,1% TFA)

	Funktion	Name oT	Datum	Unterschrift
erstellt				e.h.
geprüft-inhaltlich				e.h.
geprüft-inhaltlich				e.h.
geprüft-formal				e.h.
geprüft-formal				e.h.
freigegeben-final				e.h.

4 Verwendete Abkürzungen/ Begriffe

ACN	Acetonitril
AL	Abteilungsleitung
GalliAd	Germanium-68/Gallium-68 Radionuklid Generator
GMP	Gute Herstellungspraxis
HCl	Salzsäure
HL	Herstellleitung
HPLC	Hochdruckflüssigkeitschromatographie
HWZ	Halbwertszeit
KL	Kontrollleitung
M	Molar
MA	Mitarbeiter/in
MeOH	Methanol
Min	Minuten
mL	Milliliter
µL	Mikroliter
NaOH	Natronlauge
PET	Positronen Emissions Tomographie
pH	pH-Wert
QM	Qualitätsmanagement
Rf	Retentionsfaktor
RT	Raumtemperatur
TFA	Trifluoressigsäure
TLC	Dünnschichtchromatographie

5 Verantwortlichkeit

Für den Herstellungsprozess des Radiopharmakons [^{68}Ga]GaFAPi trägt die Herstellleitung die Verantwortung; für die ordnungsgemäße Durchführung der Qualitätskontrolle und Freigabe der Charge die Kontrollleitung des PET-Zentrums.
Die Herstellleitung garantiert die Einschulung jeder [^{68}Ga]GaFAPi produzierenden Person. Ein entsprechender Einschulungsnachweis muss im Gerätepass ausgewiesen sein: Gallium Generatoren (EZAG und GalliAd), Osmometer, pH-Meter, HPLC, TLC-Messgerät, Thermoschüttler.

6 Arbeitsablauf/Tätigkeitsbeschreibung

Synthesevorbereitung:
Die verwendeten Generatoren müssen im Zeitraum 72-4 h vor Synthesestart eluiert worden sein.
Der Thermoschüttler wird auf 30°C mindestens 5 min vor Synthesestart aufgeheizt.

Syntheseablauf:
1) 20 µL des FAPi-Precursor Aliquots (1 mg/ml Lösung) wird mit 150 µL NH_4OAc Puffer (1 M, pH 5.5) in einem 5 mL Eppendorfgefäß gemischt.
2) Die benötigten Generatoren werden in ein etikettiertes, steriles evakuiertes Gefäß eluiert.
3) 1 mL des Eluats wird mit einer Spritze (PLASTIKSPITZE!!) in die FAPi-Precursor-Mischung gegeben und das Eppi am Thermoschüttler für 15 min bei 30°C geschüttelt (700 rpm).
4) Nach der Reaktion werden 819 µL PET-Phosphatpuffer (125 mM) hinzugegeben.
5) 100 µL werden zur Qualitätskontrolle entnommen.

Qualitätskontrolle:
Die Qualitätskontrolle besteht aus der Bestimmung der radiochemischen Reinheit mit HPLC und TLC sowie der Bestimmung der physikalischen Parameter Osmolalität und pH-Wert, sowie der Halbwertzeit und dem γ-Spektrum.
Nach der Radiosynthese und der Applikation wird das Produktvial zur Endotoxin- und Sterilitätsbestimmung vollständig beschriftet abgegeben.

- (Radio)chemische Reinheitsbestimmung:

  Radio-RI-HPLC-Methode: Ga_FAPI_5M_Hannah.

  Säule: Chromolith® Performance RP-18e; 100-4.6 mm

  Flußrate: (2 mL/min)

  Rt ([^{68}Ga]FAPi): 3.4-3.7 min

  Rt ([^{68}Ga]Ga): 0.9-1.1 min

- Radio-DC:

  Rf ([^{68}Ga]FAPi): 0.9-1.1

  Rf ([([^{68}Ga]Ga-colloid): 0-0.1

- pH-Bestimmung: mit pH Meter (4.5 – 7)
- Osmolalität: mit Osmometer (200 – 400 mosmol/kg)
- Radionuklidische Reinheit: mit Gamma-Spektrometer (480-530 keV)
- Abweichungen von den Sollwerten sind dem Kontrolleiter unverzüglich mitzuteilen.

7 Erläuterungen/Weitere Informationen

Anmerkung 1: Der Precursor hat ausreichende Stabilität um gelöst in TraceSELECT® Wasser bei -20°C aufbewahrt zu werden. Dazu wird 1 mg Precursor in 1 mL TraceSELECT® Wasser gelöst und 20 µL Aliquote vorbereitet. Maximale Aufbewahrungsdauer entspricht dem Ablaufdatum am gelieferten Precursorvial.
Anmerkung 2: Während der gesamten Reaktion dürfen keine metallischen Nadeln verwendet werden.
Anmerkung 3: Keine Trennung von Produkt und freiem/kolloidalem Gallium in Citratpuffer-TLC.

8 Änderungen

Datum	Version	Änderung
24.09.2020	01	Erstellung